UNIVERSITY OF KWAZULU NATAL

ERROR PERFORMANCE ANALYSIS OF N-ARY ALAMOUTI SCHEME WITH SIGNAL SPACE DIVERSITY

Nathael Sibanda

210549566@stu.ukzn.ac.za

School of Engineering: Electrical, Electronic and Computer Engineering

Supervised by Prof Hong Jun Xu

Submitted in fulfilment of the degree of Master of Science in Engineering, College of Agriculture, Engineering and Science

School of Engineering: Electrical, Electronic and Computer Engineering, University of KwaZulu - Natal, Durban, South Africa

July 2018

EXAMINER'S COPY

Declarations

As the candidate's supervisor, I agree to the submission of this dissertation;

Date of Submission: …….

Supervisor; …….

Professor H. Xu

COLLEGE OF AGRICULTURE, ENGINEERING AND SCIENCE

DECLARATION 1 – PLAGIARISM

I, Nathael Sibanda, declare that

- The research reported in this dissertation, except where otherwise indicated, is my original research.

- This dissertation has not been submitted for any degree or examination at any other university.

- This dissertation does not contain other persons' data, pictures, graphs or other information unless specifically acknowledged as being sourced from other persons.

- This dissertation does not contain other persons' writing unless specifically acknowledged as being sourced from other researchers. Where other written sources have been quoted, then:

    a. Their words have been re-written but the general information attributed to them has been referenced
    b. Where their exact words have been used, then their writing has been placed in italics and inside quotation marks and referenced.

- This thesis does not contain text, graphics or tables copied and pasted from the Internet, unless specifically acknowledged, and the source being detailed in the thesis and in the References sections.

Signed: ……

Nathael Sibanda

July 2018

COLLEGE OF AGRICULTURE, ENGINEERING AND SCIENCE

DECLARATION 2 - PUBLICATIONS

Details of contribution to publications that form part and/or include research presented in this thesis (include publications in preparation, submitted, *in the press* and published and give details of the contributions of each author to the experimental work and writing of each publication)

Submission 1:

N. Sibanda and H. Xu. Error performance analysis of N-ary Alamouti M-QAM Scheme in Rayleigh Fading Channels. 2018.

Prepared for submission

Submission 2:

N. Sibanda and H. Xu. Error performance analysis of N-ary Alamouti M-QAM Scheme with SSD in Rayleigh Fading Channels. 2018.

Prepared for submission

Signed: ……

Nathael Sibanda

July 2018

Acknowledgements

Many thanks and my sincere gratitude to my supervisor Professor Hong Jun Xu for his patience, motivation, immense knowledge, guidance and support during my undergraduate up to MSc Engineering studies and related research. He has taught me many skills that have successfully helped me perform research. I could not have imagined having a better supervisor in my MSc studies.

Secondly, my sincere thanks also go to my brother Dr M Sibanda for giving me insightful ideas and academic counselling through my University studies from undergraduate to postgraduate level.

Thirdly, I want to thank my fellow officemates for the support, encouragement, fun and all the suffering we had in the past two years.

Finally but not least, I want to thank the almighty God for availing me of the opportunity to reach this far.

I thank you all for your part in my journey

Abstract

In this dissertation, a high-rate Alamouti scheme with Signal Space Diversity is developed to improve both the spectral efficiency and overall error performance in wireless communication links. This scheme uses high modulation techniques (M-ary quadrature amplitude modulation (M-QAM) and N-ary phase shift keying modulation (N-PSK)). Hence, this dissertation presents the mathematical models, design methodology and theoretical analysis of this high-rate Alamouti scheme with Signal Space Diversity.

To improve spectral efficiency in multiple-input multiple-output (MIMO) wireless communications an N-ary Alamouti M-ary quadrature amplitude modulation (M-QAM) scheme is proposed in this thesis. The proposed N-ary Alamouti M-QAM Scheme uses N-ary phase shift keying modulation (N-PSK) and M-QAM. The proposed scheme is investigated in Rayleigh fading channels with additive white Gaussian noise (AWGN). Based on union bound a theoretical average bit error probability (ABEP) of the system is formulated. The simulation results validate the theoretical ABEP. Both theoretical results and simulation results show that the proposed scheme improves spectral efficiency by 0.5 bit/sec/Hz in 2×4 16-PSK Alamouti 16-QAM system compared to the conventional Alamouti scheme (16-QAM).

To further improve the error performance of the proposed N-ary Alamouti M-QAM Scheme an $N_T \times N_R$ N-ary Alamouti coded M-QAM scheme with signal space diversity (SSD) is also proposed in this thesis. In this thesis, based on the nearest neighbour (NN) approach a theoretical closed-form expression of the ABEP is further derived in Rayleigh fading channels. Simulation results also validate the theoretical ABEP for N-ary Alamouti M-QAM scheme with SSD. Both theoretical and simulation results further show that the 2×4 4-PSK Alamouti 256-QAM scheme with SSD can achieve 0.8 dB gain compared to the 2×4 4-PSK Alamouti 256-QAM scheme without SSD.

Table of Contents

List of Figures

List of Tables

Notation

x	Scalar quantity x
$\|x\|$	Absolute value of x
$\mathbb{C}^{Q\times R}$	A set of $Q \times R$ complex-valued matrices
$(x)^*$	Complex conjugate of x
$\boldsymbol{x}$	Vector $\boldsymbol{x}$
$[\boldsymbol{x}]^T$	Transpose of $\boldsymbol{x}$
$\|\|\boldsymbol{x}\|\|_F$	Frobenius norm of $\boldsymbol{x}$
$(\boldsymbol{x})^H$	Hermitian (conjugate transpose) of $\boldsymbol{x}$
$*$	Convolution operator
$\approx$	Approximately equal to
$arccos(x)$	Arccosine of x
$E\{\boldsymbol{A}\}$	Statistical expectation of $\boldsymbol{A}$
$Q(\cdot)$	The Gaussian Q-function
$Re\{x\}$	Real part of a complex variable x
$\underset{x}{\text{argmin}}\ f(x)$	Value of x that minimises the function $f(x)$
$\underset{x}{\text{argmax}}\ f(x)$	Value of x that maximises the function $f(x)$
$\mathrm{d}^2(x,y)$	The squared Euclidean distance between signals x and y
$CN(\mu,\sigma^2)$	Complex Gaussian distribution with mean μ and variance σ^2

List of Acronyms

ABEP	Average Bit Error Probability
AWGN	Additive White Gaussian Noise
BER	Bit Error Rate
CSI	Channel State Information
i.i.d	Independent and Identically Distributed
LTE	Long Term Evolution
MED	Minimum Euclidean Distance
MGF	Moment Generating Function
MIMO	Multiple Input-Multiple Output
MISO	Multiple Input-Single-output
MLD	Maximum Likelihood Detection
MPD	Minimum Product Distance
N-PSK	N-ary Phase Shift Keying
M-QAM	M-ary Quadrature Amplitude Modulation
MRC	Maximal Ratio Combining
NN	Nearest Neighbour
PDF	Probability Density Function
PEP	Pairwise Error Probability
QoS	Quality-of-Service
SER	Symbol Error Rate
SISO	Single-Input Single-Output

SNR	Signal-to-Noise Ratio
SSD	Signal Space Diversity
STBC	Space-Time Block Codes
VoLTE	Voice over Long-Term Evolution
WiMax	Worldwide Interoperability for Microwave Access
5G	Fifth Generation networks

Part I

Introduction and motivation

1. Introduction

The demand for high data throughput has increased in recent wireless communication networks. Hence, future wireless communication networks are immensely supposed to be reliable with regards to high data throughput. However, physical limitations (factors that impede signal strength, speed and consistency of network connectivity) like the range and obstacles such as buildings provide a technical challenge for reliable wireless communication systems [1]. Hence this need for high-speed wireless communication has led to the demand for wireless networks to deliver higher capacities and link reliability than achieved by current systems. Various engineers have proven that the multiple-input multiple-output (MIMO) technology can improve data transfer rate, coverage and overall performance of wireless communication networks [1].

MIMO systems can be defined as the use of multiple antennas at both the transmitting and receiving ends of a wireless communication link [2]. They have been seen to introduce spatial diversity gain, spatial multiplexing gain, array gain and interference reduction in wireless communications. Spatial diversity improves the reliability of the system by combating the detrimental effects of multi-path and fading when trying to achieve high data throughput in limited-bandwidth channels. Array gain is defined as the increase in signal-to-noise (SNR) ratio in MIMO systems compared with that of single-input single-output (SISO) systems. It is a result of coherent combining of multiple signals from multiple transmitters and/ or from multiple receivers. Interference reduction in MIMO systems refers to the minimisation and/ or combating factors that impede signal strength and speed of network connectivity. Spatial multiplexing, on the other hand, provides additional data capacity by using different paths to carry additional data. The benefits of utilising MIMO systems are seen in modern wireless standards, including in IEEE 802.11n, LTE and mobile WiMAX systems, where high data rates and good link reliability are very essential [1-8].

Multipath fading may be combated using diversity techniques. Diversity techniques have been known to reduce the effect of fading and they have been seen to increase link reliability in wireless communications [1-8]. One of the most commonly used diversity techniques in MIMO systems is Alamouti space-time block coding (STBC) [9]. Alamouti STBC exploits transmit antenna diversity to better the overall diversity of a system. Alamouti scheme has both multiplexing gain and diversity gain, thus significantly increasing the channel capacity as well as improving the reliability of the wireless link [9-12].

Signal Space Diversity (SSD) is another diversity technique which offers uncoded modulation but with improvement in error performance and overall diversity of a wireless communication system [10-16]. SSD offers a better error performance without increases in the costs of adding more antennas or

extension of the bandwidth. Thus, smaller devices can be attained since the scheme does not employ any additional antennas [10-16].

This dissertation mainly focuses on the applications of MIMO technology together with diversity techniques like SSD and Alamouti STBC. More details of these schemes will now be presented.

1.1 MIMO systems

A MIMO system can be defined as a wireless communication system in which the transmitting end, as well as the receiving end, is equipped with multiple antenna elements as shown in Figure 1.1 below [1-2]. The scheme of using multiple antenna configurations instead of one is based on the idea that the signals on the transmit antennas at one end and the receive antennas at the other end, are combined in a way that the quality (error performance) or the data rate (capacity and speed) of the communication link is improved significantly [1-2].

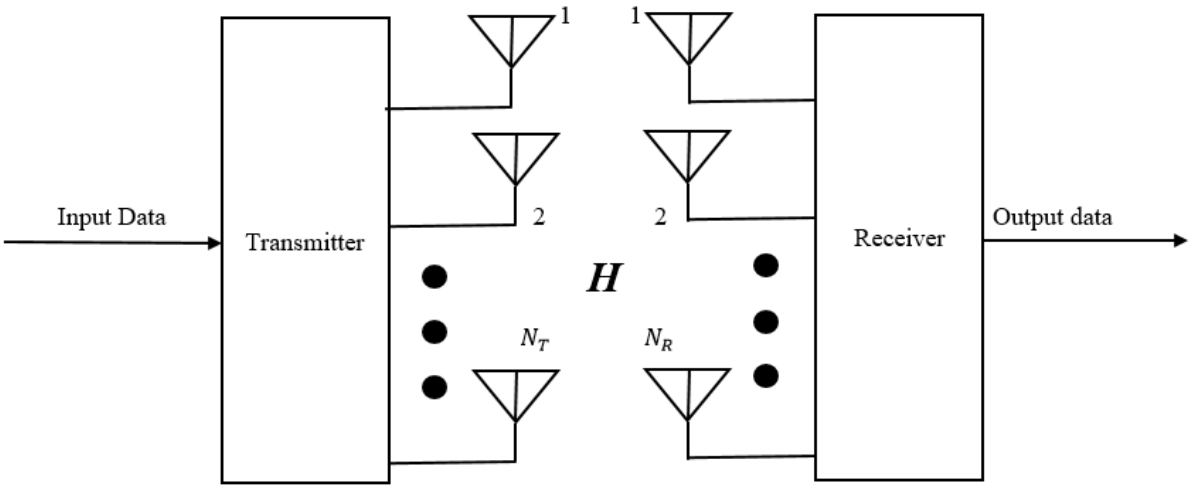

Figure 1.1: MIMO communication system.

There are two main MIMO groups namely, diversity and spatial multiplexing techniques. MIMO diversity techniques provide a higher signal-to-noise ratio (SNR) at the receiver, which improves the channel reliability, whereas MIMO spatial multiplexing linearly increases the capacity of wireless communication networks without any additional spectral resources [1-2]. In this dissertation, research was restricted to spatial multiplexing MIMO systems with diversity techniques like Signal space diversity and Alamouti-STBC to improve data rates and overall error performance of wireless communications [1-2].

1.2 Alamouti Scheme

The Alamouti scheme is a space-time block coding technique (STBC) which can achieve full diversity [2, 9-12]. The conventional Alamouti scheme with two transmit antennas and one receive antenna is illustrated in Figure 1.2 below. In Figure 1.2, $(\cdot)^*$ represents the conjugate. This is an example of a multiple-input single-output (MISO) system [14-16]. The code words of the Alamouti scheme are orthogonal and can achieve full transmit diversity specified by the number of transmitting and receiving antennas, subject to the constraint of having a simple linear decoding algorithm [2, 9-12]. Alamouti scheme in Figure 1.2, provides the same diversity order diversity as maximal ratio combing (MRC) with one transmit antenna, two receiver antennas, and a 3 dB loss in SNR with half transmission power used [2, 9-12]. In extension, the scheme may easily be generalised to a two transmit antenna and N_R receive antenna system $(2 \times N_R)$, to provide a diversity order of $2N_R$ [9-12].

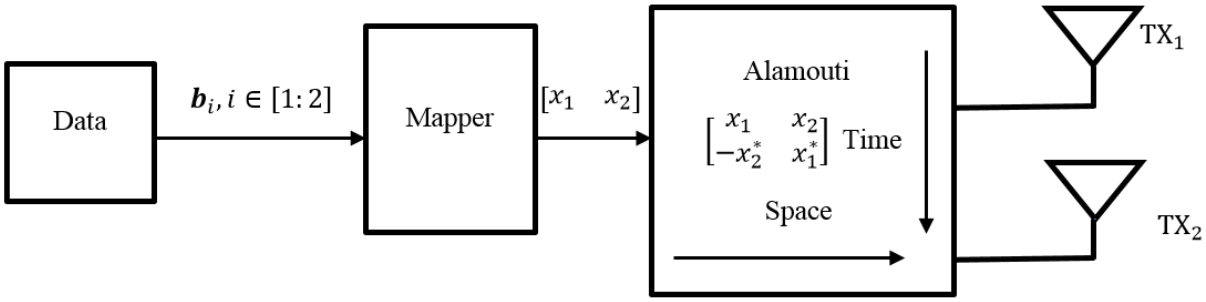

(a) Transmitter (TX)

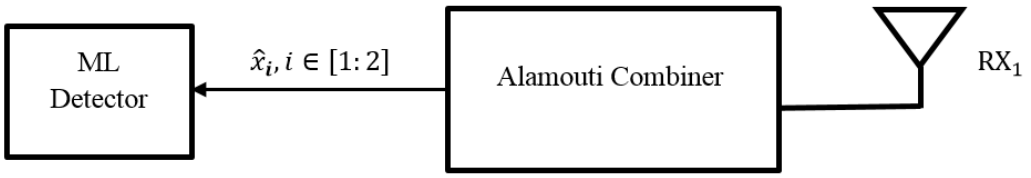

(b) Receiver (RX)

Figure 1.2: Conventional Alamouti Scheme.

The conventional Alamouti scheme takes two-time slots and it is also assumed that during each two-time slots, the channel fading remains constant but takes a different value from that of the other two time slots [2, 9-12]. Using two M-ary quadrature amplitude modulation (M-QAM) or N-ary phase shift keying (N-PSK) symbols to be transmitted, $x_i, i \in [1:2]$ with $E\{|x_i|^2\} = 1$, where $E\{\cdot\}$ denotes expectation, the block of two symbols (x_1, x_2) at the transmitter side is taken from the source and is

transmitted in the first time slot while the other pair of symbols $(-x_2^*, x_1^*)$ is transmitted in the second time slot using transmit antenna 1 and antenna 2, respectively [2, 9-12]. The encoding matrix is given by

$$\boldsymbol{X} = \begin{pmatrix} x_1 & x_2 \\ -x_2^* & x_1^* \end{pmatrix} \tag{1.2.1}$$

1.3 Signal Space Diversity

Signal Space Diversity (SSD) scheme is one of the techniques used to achieve diversity gain in fading channels. This method consists of two key operations: constellation rotation and component-wise interleaving [3, 13]. The diversity gained can only be realised after the signal points have been component interleaved [10-15]. Rotation is achieved by multiplying the constellation points with an optimum rotation angle, which increases the minimum number of distinct components between any two constellation points. Each rotated constellation's point has different in-phase (real) and quadrature (imaginary) components [3, 10-22]. After the multidimensional constellation is formed, the in-phase and quadrature components of two symbols are interleaved. This ensures that each component of the two symbols experiences independent fading so that the detector still can recover the transmitted signal even if one of the components has experienced deep fading [3, 10-22].

SSD provides signal spatial diversity, hence it improves the error performance of a communication system. Advantages of SSD include: zero additional bandwidth and zero additional transmit power required [10, 13, 20]. One of the drawbacks of SSD is that its introduction of diversity into a MIMO system brings about complexity in the maximum likelihood detection (MLD), because a more exhaustive search among all points in a rotated constellation would be required to find the transmitted symbol [14, 22-29]. An example of rotation in SSD is shown below in Figure 1.3, where a 4 QAM constellation is rotated.

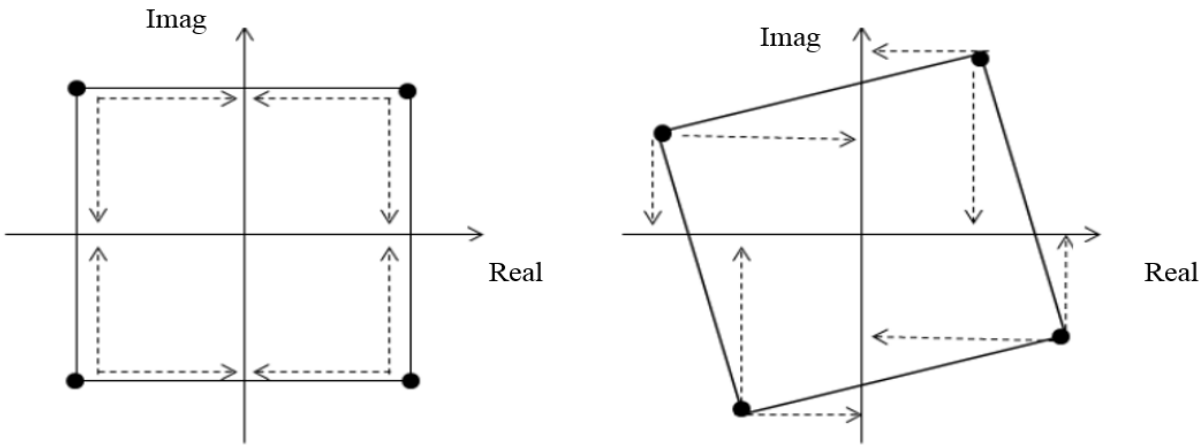

Figure 1.3: 4-QAM Constellation rotation to increase diversity order.

The process of constellation rotation in SSD is essential to the error performance of the system as it results in determining the position of the distinct components as illustrated in Figure 1.3. As the distance between the distinct components increases, the probability of error decreases and system error performance improves [13, 14, 28]. Thus determining a suitable angle of rotation which fully exploits the diversity gain is of paramount importance in SSD.

In previous literature, mainly two methods for determining the rotation angle have been discussed. One of the two methods used is the design criteria approach [10-15, 22, 28]. This method is based on rotating the constellation at an angle which ensures that every point has different in-phase and quadrature components. It is based on maximising the minimum Euclidean distance (MED) of the expanded constellation [10-15, 22, 28]. The other method used is the product distance criteria approach which is based on maximising the minimum product distance (MPD). This is the alternative approach to determining the angle of rotation by maximising the MPD, which is given in [10-15, 22, 28]. It was shown in [10-15, 22, 28] that the MPD approach results in a better overall error performance, hence in this dissertation, we apply an angle of rotation, $\theta_1 = 31.7^{\circ}$ for squared M-QAM, derived in the literature using the MPD approach.

In SSD the rotation of constellations is done using rotational matrices. In this dissertation, we use the rotational matrix shown below in equation (1.3.1) [10-15, 22, 28].

$$\boldsymbol{R}^{\theta_1} = \begin{bmatrix} \cos\theta_1 & \sin\theta_1 \\ -\sin\theta_1 & \cos\theta_1 \end{bmatrix} \tag{1.3.1}$$

where $\boldsymbol{R}^{\theta_1}$ is the rotational matrix and θ_1 is the angle of rotation according to [10-15, 22, 28].

The error performance of SSD has been evaluated using various methods in the previous literature. Two of the most used methods is the nearest neighbour (NN) approximation approach [10-15, 22, 28] and the union bound approach [22]. In this dissertation, SSD performance is evaluated using the NN approach because in [22], it was proven that the NN approximation manages better SNR performance than the union bound.

2. Motivation and Research Objective

With immense mass-market demand for mobile broadband services and the emergence of new high-capacity mobile devices (e.g. smartphones, tablets and applications), this has seen most mobile networks struggling to render high-quality consumer experience. Thus it has led to a need of clean wireless networks with uninterrupted services, good error performance and high data rates. Recent networks have relied on MIMO Alamouti based systems and error correction techniques to improve their performance, but research has shown that every bit used for error correction is a bit lost to deliver data [5-7, 24-27]. All of the afore-mentioned has brought about a great challenge to combat emerging data rate explosions in mobile networks while at the same time addressing the growing cost pressure of additional spectral resources required in wireless communications.

This section discusses the motivation of this dissertation and highlights the objectives of the research. Research has shown other MIMO Alamouti schemes that have been proposed in [24-27]. In [24], an Alamouti scheme with convolutional coding was investigated. This is where a combination of diversity transmission and forward error correction coding was used with the Alamouti scheme to improve the error performance of wireless communications. Although effective, this scheme was seen to be less effective in spectral efficiency as bits for error correction could have been maximised to deliver data. Another Alamouti scheme is seen in [25], whereby a conventional Alamouti scheme with transmit antenna selection was used with binary phase key shifting modulation to improve the error performance of wireless communications. However, this scheme was seen to be inadequate/ or less effective with bandwidth usage as it mainly improved the error performance at the expense of spectral efficiency. Hence all of this motivates an investigation of MIMO Alamouti schemes with effective diversity techniques combined with high order modulation schemes possessing a good trade-off between spectral efficiency and error performance. The schemes must also evade the challenge of the growing costs of spectrum resources.

Alamouti scheme provides effective antenna diversity using space-time block coding which introduces redundancy through multiple antennas and channel coding. Hence, combining the Alamouti scheme

and SSD with high order modulation schemes leads to high spectral efficiency and improves error performance in wireless communications. SSD exploits the spatial diversity of multi-dimensional constellations and helps to combat deep channel fading, thereby improving error performance without additional spectral resources. In addition, spectral efficiency, B_f, of MIMO wireless networks with N_T transmit antennas that send symbols from an M-ary constellation is given in [27, Section (1.2)] as

$$B_f = \frac{N_T}{\tau}\log_2(M)\ \ bits/\sec/Hz \tag{2.1}$$

where τ is the number of time slots over which the same information is transmitted.

Hence from (2.1), increasing (M) using high order modulation schemes like N-PSK and M-QAM provides a good trade-off between high spectral efficiency and improved error performance [10-12, 24-28].

In summary, the objectives of this research were to investigate and propose methods of improving spectral efficiency and error performance of MIMO Alamouti based wireless communications due to the explosion of high data rates required to support reliable communications. Hence this dissertation entails the research on two proposed Alamouti based schemes namely, the error performance analysis of N-ary Alamouti M-QAM scheme and the error performance analysis of N-ary Alamouti M-QAM scheme with SSD in Rayleigh fading channels. These are covered more in detail as the contributions to this dissertation in Part II.

3. Contributions of Included Papers

All contributions of this dissertation are presented in the form of two papers. The papers are presented in Part II of this dissertation while Part III presents concluding remarks. The details of the two papers are as follows.

3.1 Paper A

N. Sibanda and H. Xu, "Error Performance Analysis of N-ary Alamouti M-QAM Scheme in Rayleigh Fading Channels," 2018.

This paper presents N-PSK, M-QAM, and Alamouti scheme in Rayleigh fading channels. It is based on an $N_T \times N_R$ N-ary Alamouti M-ary quadrature amplitude modulation (M-QAM) scheme. The proposed N-ary Alamouti M-QAM Scheme is a Space-Time Block Coding technique (STBC) that aims to

improve spectral efficiency in multiple-input multiple-output (MIMO) wireless communications. It uses both N-ary phase shift keying modulation (N-PSK) and M-QAM. The proposed scheme's error performance is investigated in frequency-flat Rayleigh fading channels with additive white Gaussian noise (AWGN). A theoretical average bit error probability (ABEP) of the system is formulated using the union bound approach and the ABEP is validated with simulation results.

3.2 Paper B

N. Sibanda and H. Xu, " Error Performance Analysis of N-ary Alamouti Scheme with Signal Space Diversity," 2018.

In this paper, N-PSK, M-QAM, Alamouti with SSD in Rayleigh fading channels is investigated. It is based on an $N_T \times N_R$ N-ary Alamouti M-ary Quadrature Amplitude Modulation (M-QAM) scheme with Signal Space Diversity (SSD). The proposed N-ary Alamouti M-QAM Scheme is a space-time block coding technique (STBC) that aims to improve spectral efficiency and error performance in multiple-input multiple-output (MIMO) wireless communications. It uses both N-ary phase shift keying modulation (N-PSK) and M-QAM with SSD. SSD is another Diversity technique which provides Spatial Diversity with no increases in transmit power and bandwidth. SSD together with Alamouti scheme which provides full Diversity, improves the error performance at the expense of Maximum Likelihood Detection (MLD) complexity. In this study, the error performance of the proposed scheme is investigated in frequency-flat Rayleigh fading channels with additive white Gaussian noise (AWGN). A closed-form expression of the theoretical average bit error probability (ABEP) of the proposed system is formulated using the nearest neighbour (NN) approach. The theoretical ABEP together with all other deductions presented here, are validated using simulation results.

4. References

[1] A. K. Afriyie, "Multiple Input Multiple Output (MIMO) Operation Principles," Metropolia Ammattikorkeakoulu, Helsinki, Finland, 2013.

[2] A. Krumbein, "Understanding the basics of MIMO communication Technology," Southwest Antennas, Inc, San Diego, USA, 2016.

[3] J. KIm, J. Kim, W. Lee and I. Lee, "On the symbol error rates for Signal Space Diversity schemes over a Rican fading channel," *IEE Transactions on Communications,* vol. 57, no. 8, pp. 2204-2209, 2009.

[4] A. Goldsmith, Wireless communications, Cambridge : Press, 2005.

[5] A. J. Shepherd, "Sprint 4G Rollout Updates," The Wall, Washington, USA, 2012.

[6] E. Telatar, "Capacity of Multi-antenna Gaussian channels," *European Transactions on Telecommunications,* vol. 10, no. 6, pp. 558-595, 1999.

[7] S. C. Chin, "LTE-Advanced technologies on current LTE service to overcome real network problems and to increase data capacity," *IEEE ICACT,* vol. 1, pp. 275-281, 2013.

[8] P. W. Wolniansky, G. J. Foschini, G. D. Golden and R. A. Valenzuela, "V-BLAST: An architecture for realizing very high data rates over the rich-scattering wireless channel," *URSI Int. Symp, On Signals, Systems and Electronics,* no. ISSS98, pp. 295-300, 2008.

[9] S. Alamouti, "A Simple Transmit Diversity technique for wireless Communications," *IEEE, Selected Areas on Communications,* vol. 16, no. 8, pp. 1451-1458, 1998.

[10] A. Saed, H. Xu and T. Quazi, "Alamouti Space-time Block coded Hierarchical Modulation with Signal Space Diversity and MRC reception in Nakagami-m fading channels," *IET Communications,* vol. 8, no. 4, pp. 516-524, 2013.

[11] J. Taejin and C. Kyungwhoon, "Design of Concatenated Space-Time Block Codes Using Signal Space Diversity and the Alamouti Scheme," *IEEE Communications Letters,* vol. 7, no. 7, pp. 329-331, 2003.

[12] S. Jeon, J. Lee, I. Kyung and M. K. Kim, "Component-interleaved Alamouti coding with Rotated Constellations for Signal Space Diversity," *IEEE International Symposium on Broadband Multimedia Systems and Broadcasting,* vol. 1, pp. 1-6, 2010.

[13] J. Boutros and E. Viterbo, "Signal Space Diversity: A Power-and Bandwidth-efficient Diversity Technique for the Rayleigh Fading channel," *IEEE Transactions on Information Theory,* vol. 44, no. 4, pp. 1453-1467, 1998.

[14] Z. Hongjie, W. Hua, K. Jingming, F. Zesong and Y. Chaoxing, "Improved coded cooperative scheme with Signal Space Diversity in wireless networks," *IEEE on Wireless Communications and Signal processing,* vol. 1, no. WCS 2009, pp. 1-6, 2009.

[15] Seyed, A. Seyed, S. Ahmadzadeh, M. Abolfazl and K. K. Amir, "Signal Space Cooperative communication," *IEEE Transactions on Wireless Communications,* vol. 9, no. 4, pp. 1266-1271, 2010.

[16] W. Pravin and S. L. Badjate, "MIMO-Future Wireless Communication," *International Journal of Innovative Technology and Exploring Engineering (IJITEE),* vol. 2, no. 5, pp. 102-106, 2013.

[17] M. Jankiraman, Space-Time codes and MIMO systems, Boston, USA: Artech House, 2004.

[18] G. J. Foschini and M. J. Gans, "On the Limits of Wireless Communication in a Fading," *IEEE on wireless Personal communications,* vol. 6, no. 3, pp. 311-355, 1998.

[19] G. J. Foschini, "Layered Space-time architecture for wireless communication in a fading," *Bell Labs Techincal Journal,* vol. 1, no. 1, pp. 41-58, 1996.

[20] A. Chindapol, "Bit-interleaved coded modulation with Signal Space Diversity in Rayleigh fading," in *Signals, Systems and Computers Conf,* Pacific Grove, California, USA, 1999, pp. 1003-1007.

[21] L. Polak and T. Kratochvil, "Comparison of the non-rotated and rotated constellations used in DVB-T2 standard," in *Radio Elektronica International,* Bruno, USA, 2012, pp. 1-4.

[22] H. Xu and Z. Paruk, "Performance Analysis and Simplified Detection for Two-Dimensional Signal Space Diversity with MRC Reception," *SAIEE,* vol. 104, no. 3, pp. 101-102, 2013.

[23] K. K. Wong, "Performance Analysis of Single and Multiuser MIMO Diversity Channels Using Nakagami-m Distribution," *IEEE Transactions on Wireless Communications,* vol. 3, no. 4, pp. 1043-1047, 2004.

[24] J. Kaur, M. L. Singh and R. S. Sohal, "Performance of Alamouti scheme with convolution for MIMO system," in *2015 2nd International Conference on Recent Advances in Engineering & Computational Sciences (RAECS)*, Chandigarh, India, 2015.

[25] Z. Chen, J. Yuan, Z. Zhou and B. Vucetic, "Performance of Alamouti scheme with transmit antenna selection," *in Proc. 2004 IEE PIMRC,* pp. 1135-1141, 2004.

[26] C. F. Mecklenbraurer and M. Rupp, "On extended Alamouti schemes for Space-Time Coding," *WPMC,* vol. 1, no. 1, pp. 115-119, Oct. 2002.

[27] S. S. Patel, T. Quazi and H. Xu, *MSc Desertation: Performance of Enhanced Uncoded Space-Time Labelling Diversity in Realistic Channels,* Durban, South Africa, 2018.

[28] A. Essop and H. Xu, "Alamouti Coded M-QAM with Single and Double Rotated Signal Space diversity and generalised selection Combining Reception in Rayleigh Fading Channels," *SAIEE Africa Research Journal*, vol. 100, no. 3, pp. 221-223, 2015.

[29] S. A. Ahmadzadeh, "Signal Space cooperative communication," *IEEE Transactions on Wireless communications*, vol. 6, no. 4, pp. 1266-1271, 2010.

[30] N. F. Kiyani, J. H. Weber, A. G. Zajr and G. L. Stuber, "Performance Analysis of a System using Cordinate Interleaving and Constellation Rotation in Rayleigh Fading Channels," in *IEEE Conf. Veh. Tech*, Calgary, Canada, pp. 1-5, 2008.

[31] E. Viterbo and G. Taricco, "Performance of Component Interleaved Signal sets for Fading Channels," *Electronic Letters*, vol. 32, no. 13, pp. 1170-1172, 1996.

[32] N. H. Tran, H. H. Nguyen and T. Le-Ngoc, "BICM-ID with Signal Space Diversity for Keyhole Nakagami-m Fading Channels," in *Information Theory*, Nice, France, pp. 2151-2155, 2007.

[33] T. L. Jianhuua, Y. Yang and Y. Gao, "BEP Analysis for DF Cooperative Systems Combined with Signal Space Diversity," *IEEE Communication Letters*, vol. 6, no. 4, pp. 486-489, 2012.

Part II

Included Papers

Paper A

ERROR PERFORMANCE ANALYSIS OF N-ARY ALAMOUTI M-QAM SCHEME

N. Sibanda and Prof H. Xu

Abstract

This paper is based on an $N_T \times N_R$ N-ary Alamouti M-ary quadrature amplitude modulation (M-QAM) scheme. The proposed N-ary Alamouti M-QAM scheme is a space-time block coding technique (STBC) that aims to improve spectral efficiency in multiple-input multiple-output (MIMO) wireless communications. The proposed scheme uses both N-ary phase shift keying modulation (N-PSK) and M-QAM. The error performance of the proposed scheme is investigated over frequency-flat Rayleigh fading channels with additive white Gaussian noise (AWGN). A theoretical average bit error probability (ABEP) of the system is formulated using the union bound approach. The ABEP is validated with simulation results. Both theoretical results and simulation results show that the proposed scheme improves spectral efficiency by 0.5 bit/sec/Hz in 2×4 16-PSK Alamouti 16-QAM compared to the conventional Alamouti scheme (16-QAM).

A.1. Introduction

In the last decade, wireless communications have been the most popular communication industry with an exponential growth rate. As Martin Cooper had predicted in [1], the number of simultaneous voice or data connections has doubled every two and a half years (+32% per year), since the beginning of wireless communications [1-4]. This has led to a rapidly increasing demand for wireless communication systems with a high spectral efficiency and reliable link margin. Multiple-input multiple-output (MIMO) Alamouti based schemes have been seen to be an alternative solution of effectively maximising bandwidth usage and improving overall error performance of wireless communications [1-16]. MIMO systems can be defined as the use of multiple antennas at both the transmitting and receiving ends of a wireless communication network [2-3]. They are based on the idea that signals on the transmit antennas at one end and the receive antennas at the other end are combined in a way that the quality (error performance) or the data rate (capacity and speed) of the communication network is enhanced significantly [2-3].

MIMO systems have been seen to introduce either a spatial diversity gain and/ or spatial multiplexing gain in wireless communications. MIMO spatial diversity improves the channel reliability, whereas MIMO spatial multiplexing linearly increases the capacity of wireless communication networks without any additional spectral resources [2, 3, 11-12]. One of the most commonly used techniques in MIMO systems is the Alamouti scheme [2, 5, 7-10]. Alamouti scheme is a space-time block coding technique. The Alamouti scheme can achieve full diversity $(2N_R)$, where N_R is the number of receiving antennas. The Alamouti scheme also has a simple linear decoding algorithm because the code word matric of the Alamouti scheme is orthogonal [7-10].

Based on the conventional Alamouti scheme several improved MIMO-Alamouti based schemes have been presented by various researchers to improve the error performance of wireless communication networks [9-10]. In [9], Hamila and Omri proposed an improved MIMO-Alamouti STBC over highly selective fading channels for wireless communication networks. Their method was a modification of MIMO-Alamouti decoding at the receiver to adapt to channel variations and improve the link reliability of wireless communication networks. Also, another modified Alamouti scheme was proposed in [10]. The modified Alamouti algorithm is an extension of the conventional Alamouti scheme to a $2 \times N_R$ antenna system. It uses a zero forcing receiver in Rayleigh fading channels to enhance the error performance for different modulation schemes in wireless communication networks.

On the other side, various researchers have also presented theories of improving the spectral efficiency of MIMO-Alamouti STBCs [3-7]. In [7], Baloch proposed a system that improves the spectral

efficiency of MIMO-Alamouti STBCs by focusing on improving the spectral efficiency of the code unlike current methods in STBCs that focus on gaining full rate and/ or maximum diversity to improve the spectral efficiency of wireless MIMO-Alamouti STBCs. However, Tarokh [6], proved that orthogonal STBCs with more than two transmit antennas have a weakness in rate and have a high complexity decoding algorithm as the number of transmit antennas increases. Thus, [7], might not achieve full-rate orthogonal coding or maximum diversity as it has more than two multiple transmit antennas. Also, in [8], Ling and Li published work on improving the Alamouti code efficiency by expanding the modulation signal set. Unfortunately, a setback on expanding the modulation signal set is the poor bit error rate performance due to reduced minimum Euclidean distance between modulation signals.

Motivated by the published work in [8], a high-rate MIMO Alamouti STBC is proposed in this paper. The purpose of the proposed scheme is to improve the spectral efficiency of MIMO-Alamouti STBC based systems without/ or with minimum decoding complexity and retaining overall error performance.

The remainder of this paper is structured as follows: Section A.2 presents the proposed N-ary Alamouti M-QAM scheme, together with the theoretical analysis of the BER performance of the system over identical and independently distributed (i.i.d) Rayleigh frequency-flat fading channels with AWGN. Section A.3 presents the numerical results and discussion. Finally, the paper is concluded in section A.4.

Notation: For consistent notation, this paper denotes bold lowercase and uppercase letters for vectors and matrices, respectively. Regular letters represent scalar quantities. $\mathbb{C}^{Q\times R}$ is a set of $Q \times R$ complex-valued matrices. $[\cdot]^T, (\cdot)^H, (\cdot)^*, |\cdot|$and $\|\cdot\|_F$ Represent the transpose, Hermitian, conjugate, Euclidean and Frobenius norm operators, respectively.

where $Q(\cdot)$ is the Gaussian Q-function. $E\{\cdot\}$ is the expectation operator and $\mathrm{argmin}(\cdot)$ and $\mathrm{argmax}(\cdot)$ represent the argument of the minimum or maximum. Finally, $\mathrm{d}^2(x, y)$ represents the squared Euclidean distance between signals x and y.

A.2. System model

Let $\mathbf{\Omega}_1$ be the signal set of M-ary quadrature amplitude modulation (M-QAM) with a cardinality of M, and $\mathbf{\Omega}_2$ be the signal set of N-ary phase shift keying (N-PSK) with a cardinality of N.

Consider an $N_T \times N_R$ N-ary Alamouti scheme with $N_T = 2$ transmit antennas and N_R receive antennas shown in Figure A.2.1. Information bits are grouped into five bit streams $\boldsymbol{b}_i = [b_{i1} b_{i2} \cdots b_{ir}], i \in [1:4], r = \log_2 M$ and $\boldsymbol{b}_5 = [b_{51} b_{52} \cdots b_{5s}], s = \log_2 N$. Bit-stream $\boldsymbol{b}_i,\ i \in [1:4]$, is fed into a Gray-coded mapper which maps r bits into an M-QAM constellation point and yields a symbol x_i with $E\{|x_i|^2\} = 1$ while bit stream $\boldsymbol{b}_5$ is fed into another Gray-coded mapper which maps s bits into an N-PSK constellation point, and yields a symbol $x_5 = e^{\mathrm{j}\theta_q}, q \in [1:N]$ and $E\{|x_5|^2\} = 1$.

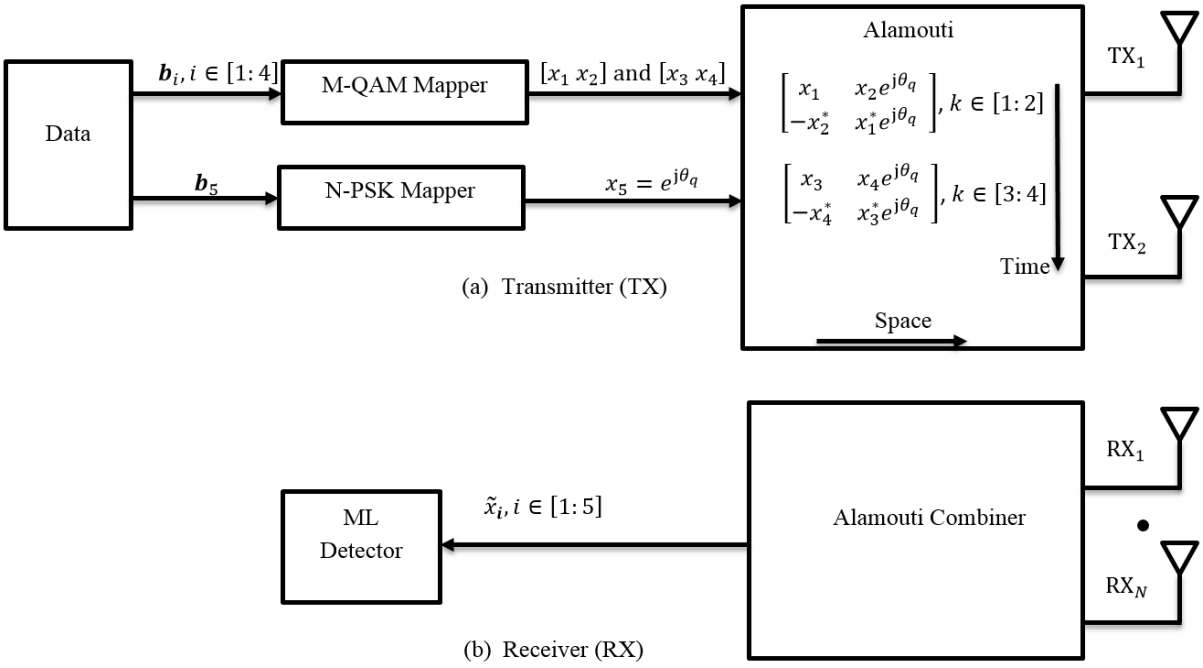

Figure A.2.1: N-ary Alamouti scheme system model.

The modified Alamouti scheme is given by

$$\boldsymbol{X}_i = \begin{bmatrix} x_{2i-1} & x_{2i} e^{\mathrm{j}\theta_q} \\ -x_{2i}^* & x_{2i-1}^* e^{\mathrm{j}\theta_q} \end{bmatrix}, i \in [1:2] \tag{A.2.1.}$$

For $\boldsymbol{X}_1$ the two pairs of symbols $\left(x_1, x_2 e^{\mathrm{j}\theta_q}\right)$ and $\left(-x_2^*, x_1^* e^{\mathrm{j}\theta_q}\right)$ are transmitted through transmit antenna one and two in the first two time slots while for $\boldsymbol{X}_2$, the other two pairs of symbols $\left(x_3, x_4 e^{\mathrm{j}\theta_q}\right)$ and $\left(-x_4^*, x_3^* e^{\mathrm{j}\theta_q}\right)$ are transmitted in the second two time slots. We refer to the above transmission scheme as N-ary Alamouti M-QAM scheme.

The received signals are given by

$$\boldsymbol{y}_{2v-1} = \boldsymbol{h}_{2v-1} x_{2v-1} + \boldsymbol{h}_{2v} x_{2v} e^{\mathrm{j}\theta_q} + \boldsymbol{n}_{2v-1}, v \in [1:2] \tag{A.2.2}$$

$$\boldsymbol{y}_{2v} = \boldsymbol{h}_{2v-1}(-x_{2v}^*) + \boldsymbol{h}_{2v} x_{2v-1}^* e^{\mathrm{j}\theta_q} + \boldsymbol{n}_{2v}, v \in [1:2] \tag{A.2.3}$$

where $\boldsymbol{y}_l \in \mathbb{C}^{N_R \times 1}$ is the l^{th} received signal vector, $\boldsymbol{h}_l \in \mathbb{C}^{N_R \times 1}$ is the l^{th} channel fading vector, and $\boldsymbol{n}_l \in \mathbb{C}^{N_R \times 1}$ is the l^{th} received additive white Gaussian (AWGN) noise vector. It is assumed that $\boldsymbol{h}_l$ is a quasi-static frequency flat-Rayleigh fading channel. $\boldsymbol{h}_l$ remains the same value in two-time slots and takes an independent value in another two-time slots. The entries of $\boldsymbol{n}_l$ and $\boldsymbol{h}_l$ are independent and identically distributed (i.i.d) Gaussian random variables (RVs) with distribution $CN(0,2/\rho)$, $CN(0,1)$ respectively. $\frac{\rho}{2}$ is the average signal-to-noise ratio (SNR) at each receive antenna [22-26].

A.2.2. Detection

Based on [7-9, 19], it is assumed that full channel state information (CSI) is known at the receiver and the detection process is done using the following steps.

Step 1: Given $x_5 = e^{\mathrm{j}\theta_q}$, $q \in [1: N]$, the received signals in (A.2.2) and (A.2.3) are sent to the combiner and the output of the combiner is given by;

$$\tilde{Z}_{2w-1}(x_5) = (\boldsymbol{h}_{2w-1}^H)(\boldsymbol{y}_{2w-1}) + (\boldsymbol{y}_{2w}^H)(\boldsymbol{H}_{2w}),\ w \in [1:2] \tag{A.2.4}$$

$$\tilde{Z}_{2w}(x_5) = (\boldsymbol{H}_{2w}^H)(\boldsymbol{y}_{2w-1}) - (\boldsymbol{y}_{2w}^H)(\boldsymbol{h}_{2w-1}), w \in [1:2] \tag{A.2.5}$$

where $w \in [1:2]$, $\boldsymbol{H}_{2w} = \boldsymbol{h}_{2w} e^{\mathrm{j}\theta_q}$ and $\tilde{Z}_l \in \mathbb{C}^{1\times 1}, l \in [1:4]$ are the outputs of the combiner.
(A.2.4) and (A.2.5) can be further rewritten as

$$\tilde{Z}_{2w-1}(x_5) = (\|\boldsymbol{h}_{2w-1}\|_F^2 + \|\boldsymbol{h}_{2w}\|_F^2)x_{2w-1} + \tilde{n}_{2w-1},\ w \in [1:2] \tag{A.2.6}$$

$$\tilde{Z}_{2w}(x_5) = (\|\boldsymbol{h}_{2w-1}\|_F^2 + \|\boldsymbol{h}_{2w}\|_F^2)x_{2w} + \tilde{n}_{2w},\ w \in [1:2] \tag{A.2.7}$$

Step 2: The outputs of the combiner from (A.2.6) and (A.2.7) are then sent to the estimator where the N-PSK and M-QAM symbols decoupling and estimation process happens [19-21, 23]. Thus, for each given N-PSK symbol $x_5 = e^{\mathrm{j}\theta_q}$, the four transmitted M-QAM symbols are detected first and the estimated four candidate symbols $\big(\hat{x}_i(x_5)\big), i \in [1:4]$ are given as;

$$\hat{x}_{2w-1}(x_5) = D\big(U_{2w-1}(x_5)\big), w \in [1:2], \tag{A.2.8}$$

$$\hat{x}_{2w}(x_5) = D\big(U_{2w}(x_5)\big), w \in [1:2] \tag{A.2.9}$$

where $U_{2w-1}(x_5) = \frac{\tilde{Z}_{2w-1}(x_5)}{g_{2w-1}(x_5)}$, $U_{2w}(x_5) = \frac{\tilde{Z}_{2w}(x_5)}{g_{2w}(x_5)}$, $g_{2w-1}(x_5) = (\|\boldsymbol{h}_{2w-1}\|_F^2 + \|\boldsymbol{h}_{2w}\|_F^2)$ and $g_{2w}(x_5) = (\|\boldsymbol{h}_{2w-1}\|_F^2 + \|\boldsymbol{h}_{2w}\|_F^2),\ w \in [1:2]$. $D(\cdot)$ denotes an M-QAM demodulation function.

Step 3: The four estimated M-QAM symbols are assumed to be correctly detected and the following metric distance $\left(\mathrm{P}(\,x_5)\right)$, is calculated using $\hat{x}_i(\,x_5), i \in [1:4]$ and the given $x_5 = e^{\mathrm{j}\theta_q}$ value to obtain;

$$\mathrm{P}(\,x_5) = \sum_{i=1}^{4} d_i\,(\,x_5),\ i \in [1:4] \tag{A.2.10}$$

where $d_{2i-1}(\,x_5) = \left\|\boldsymbol{y}_{2i-1} - (\boldsymbol{h}_{2i-1})\left(\hat{x}_{2i-1}(\,x_5)\right) - (\boldsymbol{h}_{2i})\left(\hat{x}_{2i}(\,x_5)\right)(\,x_5)\right\|_F^2,\ i \in [1:2]$

and $d_{2i}(\,x_5) = \left\|\boldsymbol{y}_{2i} - (\boldsymbol{h}_{2i-1})\left(-\hat{x}_{2i}^*(\,x_5)\right) - (\boldsymbol{h}_{2i})\left(\hat{x}_{2i-1}^*(\,x_5)\right)(\,x_5)\right\|_F^2,\ i \in [1:2]$

Step 4: Steps 1 up to 3 are run repeatedly *N* times and hence, *N* values of the distances $\mathrm{P}_i(\,x_5)$, are obtained and stored in a $1 \times N$ matrix ($\mathbf{F}(\,x_5)$).

Step 5: Finally, the estimation of the N-PSK symbol $\tilde{x}_5$ is done by minimising the following ML metric.

$$\tilde{x}_5 = \underset{e^{\mathrm{j}\theta_q},\tilde{x}_i=\hat{x}_i(\,x_5)\in\boldsymbol{\Omega}_3}{\operatorname{argmin}} \left(\mathbf{F}(\,x_5)\right),\ i \in [1:4] \tag{A.2.11}$$

where $\tilde{x}_5 = e^{\mathrm{j}\hat{\theta}_q}$ is the estimation of the N-PSK symbol and $\boldsymbol{\Omega}_3$ is the set containing the estimated M-QAM symbols $\hat{x}_i, i \in [1:4]$ and the given $\left(\,x_5 = e^{\mathrm{j}\theta_q}\right)$ value.

A.2.3. Error Performance Analysis

The detection discussed in the previous section actually is a joint detection. There are two types of errors in the above detection. One is the error of estimating the N-PSK symbol while the other one is the error in estimating M-QAM symbols. It is difficult to derive the whole error probability of the joint detection. In this section, we only consider the low error performance bound of the joint detection. That is, we only consider the error probability of estimating M-QAM symbols given that the N-PSK symbol is perfectly detected. Let P_d denote the average bit error probability (ABEP) of estimating M-QAM symbols given that the M-PSK symbol is perfectly detected. The low error probability bound of the proposed system is given by

$$P_e \geq P_d \tag{A.2.12}$$

Given that the N-PSK symbol $\left(e^{\mathrm{j}\theta_q}\right)$ is perfectly detected at the receiver then the equivalent received signal may be written as

$$\boldsymbol{y}_{2v-1} = \boldsymbol{h}_{2v-1}x_{2v-1} + \boldsymbol{H}_{2v}x_{2v} + \boldsymbol{n}_{2v-1},\ v \in [1:2] \quad \text{(A.2.13)}$$

$$\boldsymbol{y}_{2v} = \boldsymbol{h}_{2v-1}(-x_{2v}^{*}) + \boldsymbol{H}_{2v}x_{2v-1}^{*} + \boldsymbol{n}_{2v},\ v \in [1:2] \quad \text{(A.2.14)}$$

where $\boldsymbol{H}_{2v}, v \in [1:2]$ are known at the receiver.

N-ary Alamouti M-QAM may be viewed as a $2 \times N_R$ MIMO configuration, as it resembles a MIMO system with two transmit antennas and N_R receivers. In [14, 29], it was shown that an Alamouti scheme with N_R receive antennas is equivalent to an MRC system with $2N_R$ receive antennas and half transmission power used. Hence the ABEP of M-QAM symbols for N-ary Alamouti M-QAM in terms of MRC reception over Rayleigh fading channels is given by [21-22] as;

$$P_d(\rho) = \frac{a}{n\,r}\left\{\frac{1}{2}\left(\frac{2}{2+b\rho}\right)^{2N_R} - \frac{a}{2}\left(\frac{1}{1+b\rho}\right)^{2N_R} + (1-a)\sum_{i=1}^{n-1}\left(\frac{S_i}{S_i+b\rho}\right)^{2N_R} + \sum_{i=n}^{2n-1}\left(\frac{S_i}{S_i+b\rho}\right)^{2N_R}\right\} \quad \text{(A.2.15)}$$

where $a = \left(1 - \frac{1}{\sqrt{M}}\right), b = \frac{3}{M-1}$, $S_i = 2(\sin\beta_i)^2$, $\beta_i = \frac{i\pi}{4n}$ and n is the number of summations for convergence.

A.3. Results and Discussion

The aim of this section was to validate the analytical performance developed in eq (A.2.15) and then provide an error performance comparison between the various N-ary Alamouti M-QAM schemes. Monte Carlo simulations were performed over i.i.d Rayleigh flat fading channels with AWGN, where the ABEP was plotted against the average SNR at each receive antenna. The parameters regarding the AWGN and channels were consistent with those defined in section A.2.1-2. The following were assumed during the simulation: Gray coded M-QAM and Gray coded N-PSK constellations; full CSI at the receivers; transmit and receive channels were separated wide enough to avoid correlation and total transmit power was the same for all transmissions.

Figures A.3.1 - A.3.2 show the analytical and simulated ABEP of the 2×2 and 2×4 N-ary Alamouti 16-QAM systems together with the 2×2 and 2×4 Alamouti 16-QAM without N-PSK systems. In the 2×4 results, the theoretical results closely predict the BER performance in the high SNR region. (4-PSK and 8-PSK) Alamouti 16-QAM simulated results increasingly match the theoretical results in the high SNR region. It can also be shown that 2×4 (4-PSK and 8-PSK) Alamouti 16-QAM systems have closely the same BER performance as the standard 2×4 Alamouti 16-QAM without N-PSK systems. However, the proposed scheme has higher spectral efficiency as compared to the standard $2 \times$

4 Alamouti 16-QAM without PSK systems. The proposed scheme has more data throughput with five symbols sent (more bits sent) whereas the standard 2×4 Alamouti 16-QAM without N-PSK systems have only four symbols sent (fewer bits sent). An example of improved spectral efficiency is seen in 16-PSK Alamouti 16-QAM, which has a high spectral efficiency of 1.5 bits/sec/Hz as compared to 1 bit/sec/Hz 16-QAM Alamouti scheme. These values were calculated with the aid of eq (2.1) and Table A.3.2, where $N_T = 2, \tau = 4$ and the number of bits depends on the system concerned (4 bits for 16-QAM Alamouti scheme and 8 bits for 16-PSK Alamouti 16-QAM). However, it can also be seen from the results that BER performance improves with the increasing number of receivers. This is seen from the 2×2 results of the 4-PSK Alamouti 16-QAM where the theoretical does not closely match the simulated results as compared to the 2×4 results and there is evidence at 16 dB SNR of an improvement in BER of 1.2188×10^{-5} in the 2×4 system as compared to a BER of 1.4443×10^{-3} at the same SNR in the 2×2 system.

The next set of results (Figures A.3.3 - A.3.6), show the analytical and simulated ABEP of the 2×2 and 2×4 N-ary Alamouti 64 and 256-QAM systems together with the 2×2 and 2×4 Alamouti 64 and 256-QAM without N-PSK systems. Included in Figures A.3.5 – A.3.8, are the 16 PSK Alamouti 64 and 256-QAM results. These results exhibit the same characteristics as those of Figures A.3.1– A.3.2. 16-PSK Alamouti 64 and 256-QAM simulated results closely match their corresponding theoretical results with increasing SNR. Also, the results show more data throughput in 16-PSK Alamouti 64 and 256-QAM as compared to the Alamouti 64 and 256-QAM without N-PSK systems. An example of improved spectral efficiency is seen in 16-PSK Alamouti 64-QAM scheme where an increase in spectral efficiency of 1.7 bits/sec/Hz as compared to 1.3 bits/sec/Hz of 64-QAM Alamouti without N-PSK is seen. These values were calculated with the aid of eq (2.1) and table A.3.3, where $N_T = 2, \tau = 4$ and the number of bits depends on the system concerned (6 bits for 64-QAM Alamouti scheme and 10 bits for 16-PSK Alamouti 64-QAM). Thus, improved bandwidth efficiency in the proposed N-ary Alamouti M-QAM scheme.

However, it can also be seen from the results that the BER performance improves with the increasing number of receivers and modulation order. Multiple receivers and higher modulation orders mean more receive diversity as they increase the signal-to-noise-ratio at the destination. This, in turn, leads to an improved error performance [32]. This is seen from the 2×2 results where the theoretical does not closely match the simulated results and has a poor error performance as compared to the 2×4 results. The evidence is seen in the 2×2 16-QAM results where there is a BER of 1×10^{-4} at 20 dB compared to a BER of 4.7×10^{-8} at 20 dB of the 2×4 16-QAM results.

Table A.3.4: N-ary Alamouti spectral efficiency values.

QAM constellation	PSK constellation	Standard Alamouti bits sent	N-ary Alamouti bits sent	Standard Alamouti spectral efficiency (bits/sec/Hz)	N-ary Alamouti spectral efficiency (bits/sec/Hz)
16	4	4	6	1	1.3
16	8	4	7	1	1.4
16	16	4	8	1	1.5
32	4	5	7	1.2	1.4
32	8	5	8	1.2	1.5
32	16	5	9	1.2	1.6
64	4	6	8	1.3	1.5
64	8	6	9	1.3	1.6
64	16	6	10	1.3	1.7
256	4	8	10	1.5	1.7
256	8	8	11	1.5	1.7
256	16	8	12	1.5	1.8

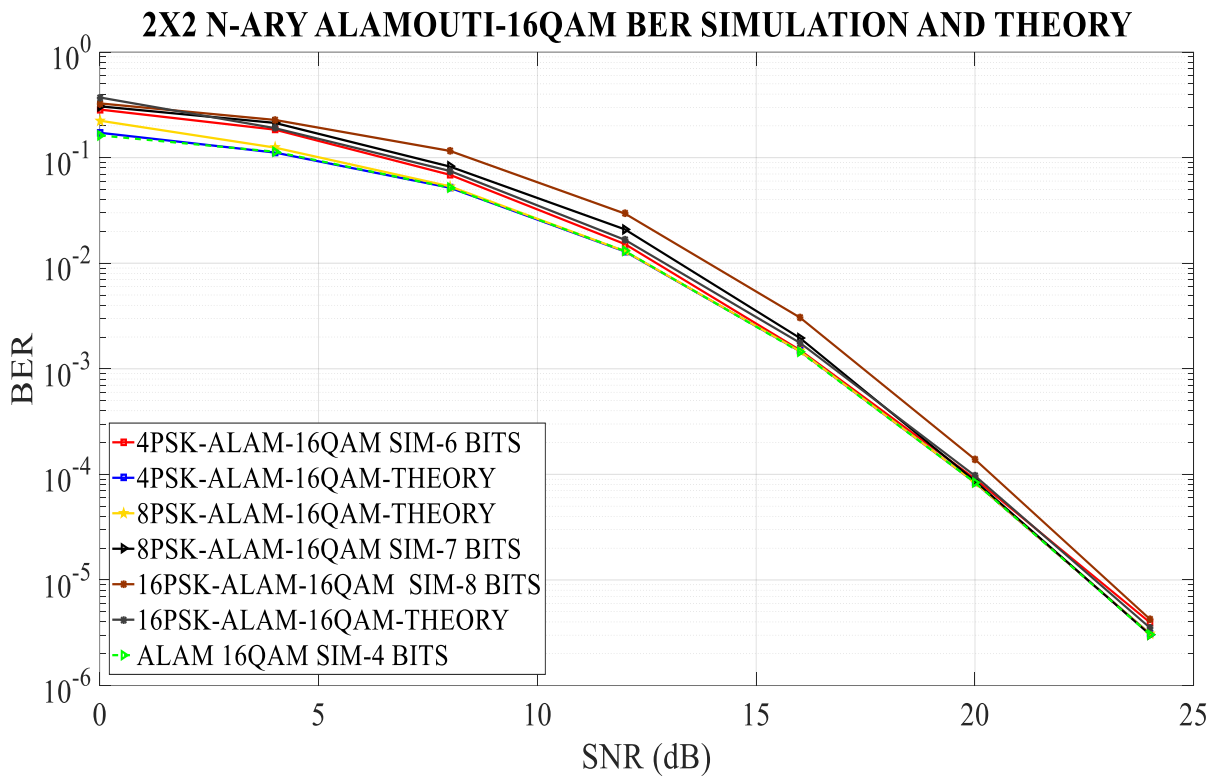

Figure A.3.1: 2×2 N-ary Alamouti 16-QAM Results.

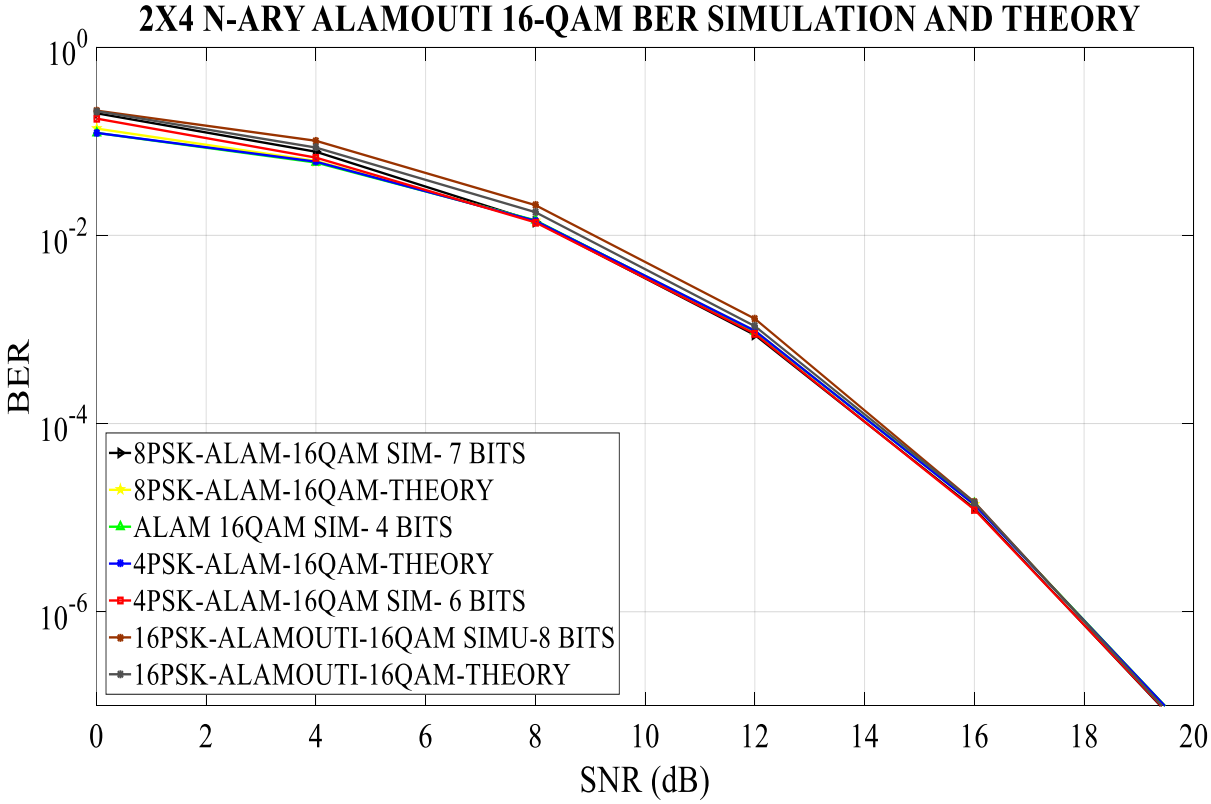

Figure A.3.2: 2 × 4 N-ary Alamouti 16-QAM Results.

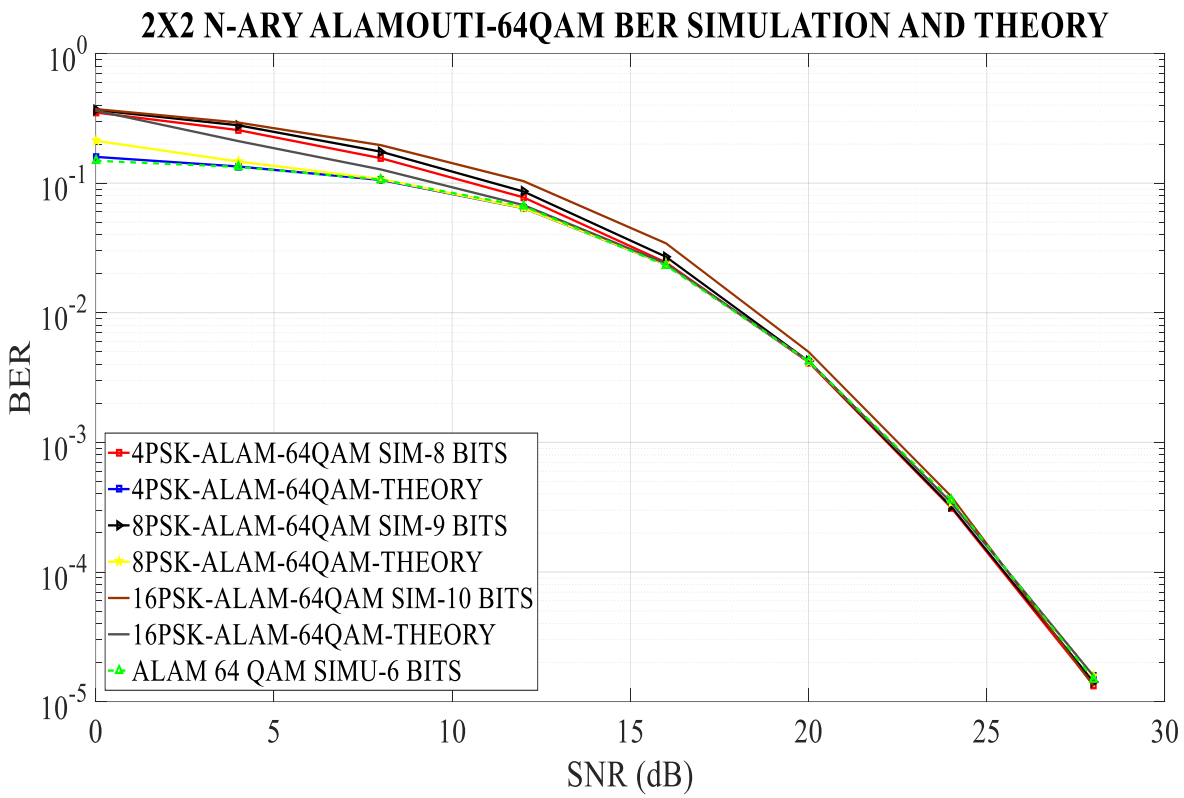

Figure A.3.3: 2×2 N-ary Alamouti 64-QAM Results.

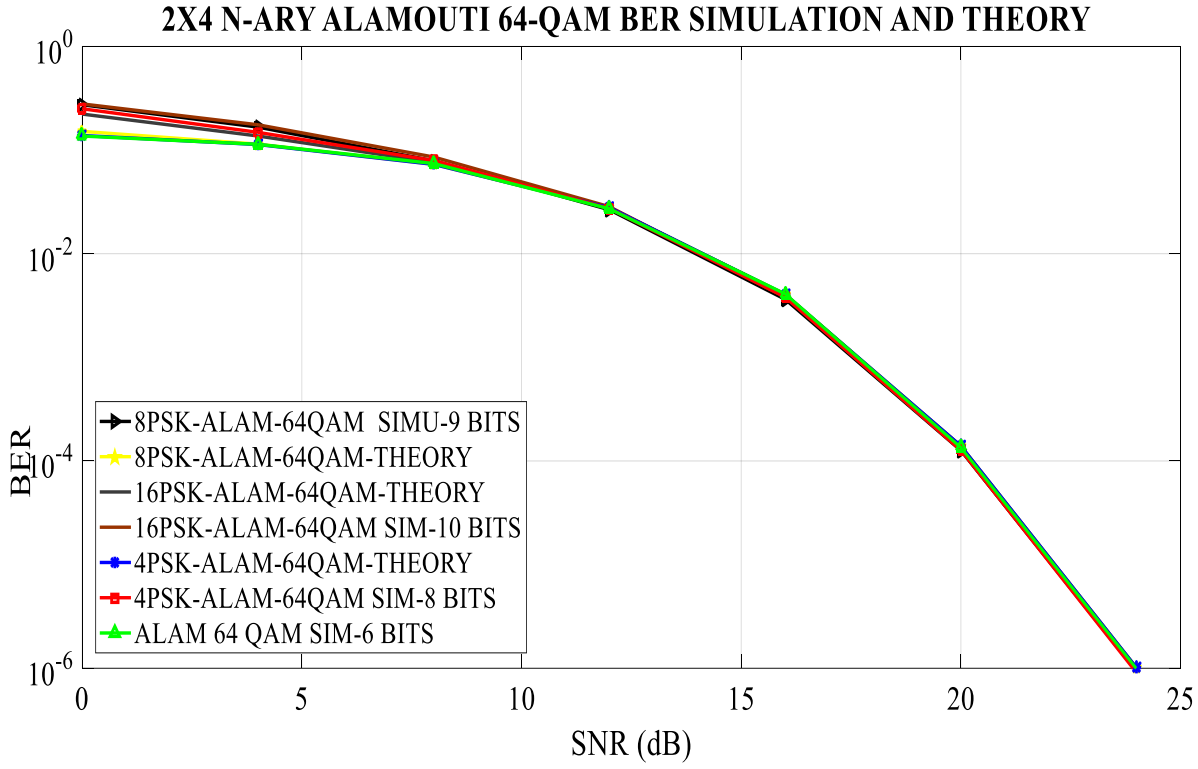

Figure A.3.4: 2×4 N-ary Alamouti 64-QAM Results.

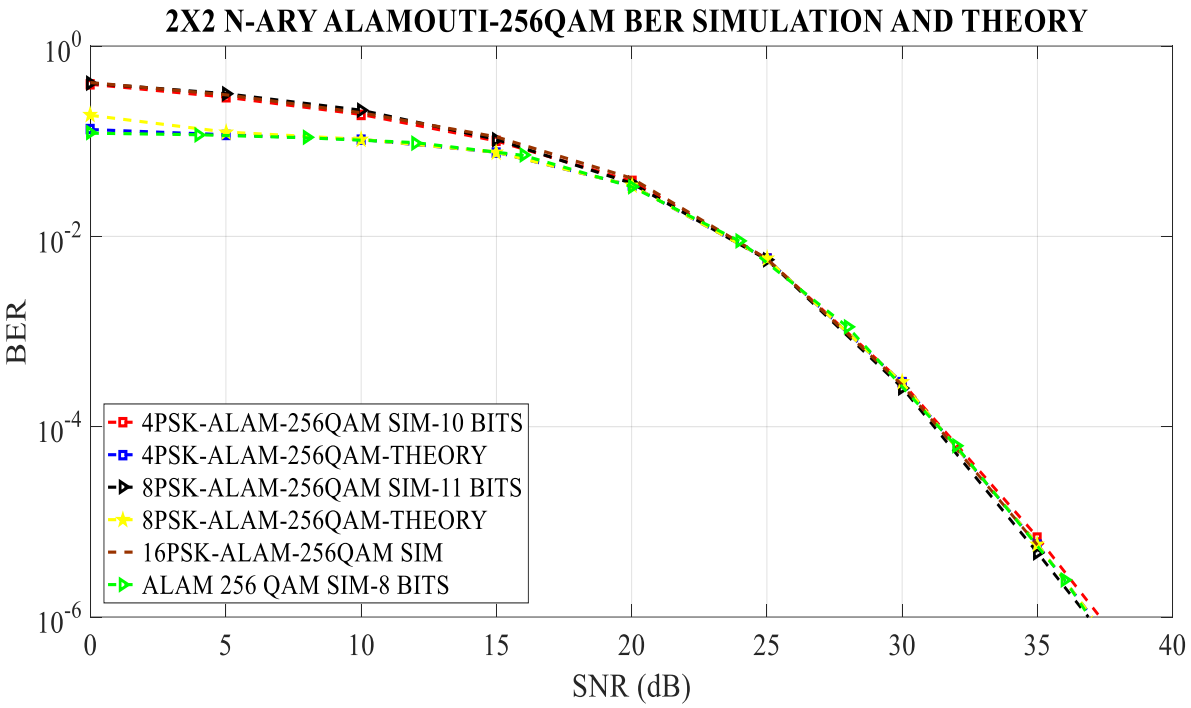

Figure A.3.5: 2×2 N-ary Alamouti 256-QAM Results.

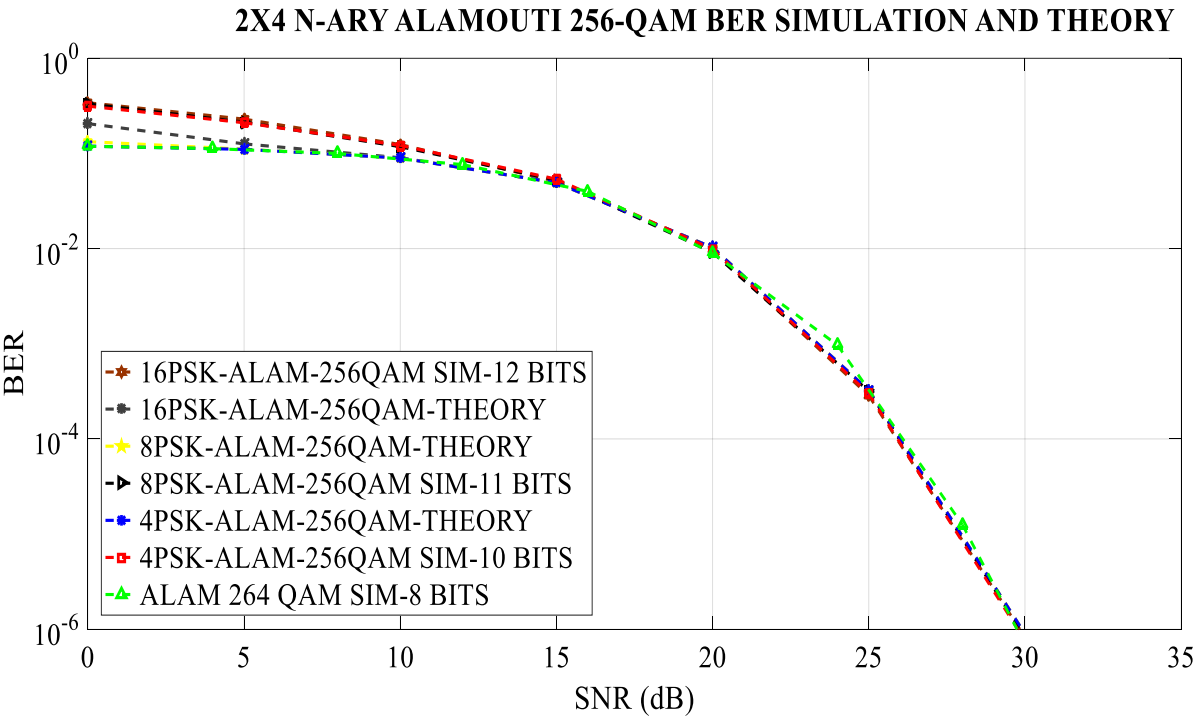

Figure A.3.6: 2×4 N-ary Alamouti 256-QAM Results.

A.4. Conclusion

In this paper, the impact of impaired performance (poor BER performance) and spectral inefficiency of Alamouti systems was investigated. The study was restricted to 2×2 and 2×4 systems of (4, 8 and 16-PSK) Alamouti (16, 64 and 256 QAM) schemes. An analytical ABEP expression was derived and validated against simulated results. The analytical results were seen to converge to simulation results in the high SNR region. The results presented, indicated increased spectral efficiency in the proposed scheme but with closely the same BER performance as standard 2×4 Alamouti M-QAM systems. Thus the proposed N-ary Alamouti M-QAM scheme has more bandwidth efficiency as compared to standard M-QAM Alamouti scheme. Also, it was found that the BER performance improved with the increase in the number of receivers.

A.5. References

[1] A. Ygomi, "Array Com-Excellence in Wireless broadband," 2011. [Online]. Available: http://www.arraycomm.com/technology/coopers-law/. [Accessed 4 February 2018].

[2] A. A. Kwabena, *Multiple Input Multiple Output (MIMO) Operation Principles,* Finland: Helsinki Metropolia University Of Applied Sciences, Thesis published, 2013.

[3] A. Krumbein, "White Paper: Understanding the basics of MIMO communication Technology," 1 November 2016. [Online]. Available: https://www.southwestantennas.com/white-paper-understanding-basics-mimo-communication-technology. [Accessed 16 February 2018].

[4] G. J. Foschini, "Layered Space-time architecture for wireless communication in a fading," *Bell Labs Techincal Journal,* vol. 1, no. 1, pp. 41-58, 1996.

[5] B. Dlodlo and H. Xu, "Bandwidth Efficiency Improvement for Differential Alamouti Space-time Block Codes using M-QAM," *SAIEE Africa Research Journal,* vol. 109, no. 4, pp. 217-223, 2018.

[6] V. Tarokh, H. Jafarkhani and A. R. Calderbank, "Space-time Block Codes from Orthogonal Designs," *IEEE Transactions On Information Theory,* vol. 45, no. 5, pp. 1456-1467, 1999.

[7] Z. A. Baloch, M. U. Baloch and N. Hussain, "Efficiency improvement of space-time block codes," *International Journal of Coomun Net and Syst Sci,* vol. 3, no. 6, pp. 507-510, 2010.

[8] Q. Ling and T. Li, "Efficiency improvement for Alamouti codes," in *IEEE 40th Annual Conference on Information Sciences and Systems,* Princeton, New Jersey, USA, pp. 569-572. 2006.

[9] R. Hamila, M. O. Hasna and R. Bouallegue, "Modified Alamouti Decoding for Highly Selective channels for LTE systems," *IEEE ISSPA,* vol. 1, no. 1, pp. 140-944, 2012.

[10] R. Kalaiyarasan and D. Saraswady, "Optimal performance in MIMO System using Modified Alamouti Algorithm," 1 October 2015. [Online]. Available: https://ieeexplore.ieee.org/stamp/stamp.jsp?tp=&arnumber=7282318. [Accessed 28 February 2018].

[11] T. L. Marzetta and B. M. Hochwald, "Capacity of a mobile multi-antenna communication link in Rayleigh Fading," *IEEE Tansactions On Information Theory,* vol. 45, no. 1, pp. 139-157, 1999.

[12] C. Oestges and B. Clerckx, MIMO Wireless Communications: From Real-world propagation to Space-Time Code design, Amsterdam, Netherlands: Elsevier, 2007Amsterdam, Netherlands.

[13] J. G. Proakis, Digital Communications, New York: McGraw-Hill, 2001.

[14] H. Xu, "Symbol Error Probability for Generalised Selection Combining Reception of M-QAM," *SAIEEE Africa Research Journal,* vol. 100, no. 3, pp. 68-71, 2009.

[15] J. Horst and B. Bessai, MIMO Signal and Systems, Springer, Germany: Springer Science H-Business Media, 2005.

[16] H. Bolcskei, D. Gesbert, C. Papadias and A. J. Van der Veen, Space-Time Wireless Systems: From Array Processing to MIMO Communications, Cambridge, UK: Press, 2006.

[17] H. Bolcskei and A. J. Paulraj, Multiple Input Multiple Output (MIMO) wireless systems, CRC: Press, 2002.

[18] K. K. Wong, "Performance Analysis of Single and Multiuser MIMO Diversity Channels Using Nakagami-m Distribution," *IEEE Transactions on Wireless Communications,* vol. 3, no. 4, pp. 1043-1047, 2004.

[19] S. Alamouti, "A Simple Transmit Diversity technique for wireless Communications," *IEEE, Selected Areas on Communications,* vol. 16, no. 8, pp. 1451-1458, 1998.

[20] A. Saed, H. Xu and T. Quazi, "Alamouti Space-time Block coded Hierarchical Modulation with Signal Space Diversity and MRC reception in Nakagami-m fading channels," *IET Communications,* vol. 8, no. 4, pp. 516-524, 2013.

[21] A. Essop and H. Xu, "Alamouti Coded M-QAM with Single and Double Rotated Signal Space Diversity and generalised selection Combining Reception in Rayleigh Fading Channels," *SAIEE Africa Research Journal,* vol. 100, no. 3, pp. 221-223, 2015.

[22] H. Xu and Z. Paruk, "Perfomance Analyisi and Simplified Detection for Two-Dimensional Signal Space Diversity with MRC Reception," *SAIEE,* vol. 104, no. 3, pp. 101-102, 2013.

[23] J. H. Winters, "The Diversity gain of Transmit Diversity in wireless systems with Rayleigh Fading," *IEEE ICC,* vol. 2, no. 1, pp. 1121-1125, 1994.

[24] N. Seshadri, "Two Signallling schemes for improving the error performance of FDD transmission systems using transmitter Diversity," *IEEE Vehicular Techonology,* vol. 1, no. 1, pp. 508-511, 1993.

[25] M. Rindani and N. Rindani, "Perfomance improvement of 4X4 Extended Alamouti Scheme with implementation of Eigen Beamforming," *IJCA*, vol. 119, no. 1, pp. 975-1000, 2015.

[26] M. Panthania and V. Bhatia, "BER Aanalysis of STBC Alamouti's Code for MIMO Sytems," *SSRG-IJECE*, vol. 2, no. 7, pp. 2348-2354, 2015.

[27] H. Haas, W. Ahn, S. Yun and R. Mesleh, "Spatial modulation-A new low-complexity spectral efficiency enhancing technique," in *CHINACOM*, Beijing, China, October, pp. 1-5. 2006.

[28] R. Mesleh, H. Haas, S. Sinanovic, S. Ahn and S. Yun, "Spatial modulation," *IEEE Transactions on Vehicular Technology*, vol. 57, no. 4, pp. 2228-2241, 2008.

[29] J. Jeganathan, A. Ghrayeb and L. Szczecinski, "Spatial Modulation: Optimal Detection and Performance Analysis," *IEEE Commun Letters*, vol. 12, no. 8, pp. 545-547, 2008.

[30] J. Taejin and C. Kyungwhoon, "Design of Concatenated Space-Time Block Codes Using Signal Space Diversity and the Alamouti Scheme," *IEEE Communications Letters*, vol. 7, no. 7, pp. 329-331, 2003.

[31] S. Jeon, J. Lee, I. Kyung and M. K. Kim, "Component-interleaved Alamouti coding with Rotated Constellations for Signal Space Diversity," *IEEE International Symposium on Broadband Multimedia Systems and Broadcasting*, vol. 1, no. 1, pp. 1-6, 2010.

[32] S. Tarun, I. Kaur and B. Pahwa, "Simplified processing for high-efficiency wireless communication employing multiple antenna aarays," *IJCA*, vol. 87, no. 16, pp. 31-35, 2014.

[33] L. Tran, T. Wysocky, A. Mertins and J. Seberry, Complex Orthogonal Space-time Processing in Wireless Communications, New York: Springer-Verlag, 2006.

[34] I. AL-Shahrani, "Performance of M-QAM Over generalised Mobile Fading Channels Using MRC Diversity," MSc Published Thesis, King Saud University, RIA, Saudi Arabia, 2007.

[35] S. Jeon, I. Kyung and M. S. Kim, "Component-Interleaved Receive MRC with Rotated Constellation for Signal Space Diversity," in *70th IEEE Semi-Annual Vehicular Technology Conference (IEEE VTC 2009- Fall)*, Anchorage, Alaska, USA, September, 2009.

[36] N. F. Kiyani, J. H. Weber, A. G. Zajr and G. L. Stuber, "Performance Analysis of a System using Cordinate Interleaving and constelation Rotation in Rayleigh Fading Channels," in *IEEE Conference Vehicular Technonology*, Calgary, Canada, pp. 1-5, 2008.

Paper B

ERROR PERFORMANCE ANALYSIS OF N-ARY ALAMOUTI SCHEME WITH SIGNAL SPACE DIVERSITY

N. Sibanda and H. Xu

Abstract

An $N_T \times N_R$ N-ary Alamouti M-ary quadrature amplitude modulation (M-QAM) scheme with signal space diversity is proposed in this paper. The proposed N-ary Alamouti M-QAM with signal space diversity (SSD) scheme is a space-time block coding technique (STBC) that aims to improve both spectral efficiency and error performance of multiple-input multiple-output (MIMO) wireless communications. It uses both N-ary phase shift keying modulation (N-PSK) and M-QAM with SSD. SSD together with Alamouti scheme which provides full diversity, improves the error performance at the expense of Maximum Likelihood Detection (MLD) complexity. In this study, the error performance of the proposed scheme is investigated over frequency-flat Rayleigh fading channels with additive white Gaussian noise (AWGN). A closed-form expression of the theoretical average bit error probability (ABEP) of the proposed system is formulated using the nearest neighbour (NN) approach based on the minimum Euclidean distance (ED). The theoretical ABEP together with all other deductions presented here, is validated using simulation results. Both the theoretical and simulation results prove that the proposed scheme improves spectral efficiency and error performance (0.8 dB improvement at a BER of 1.06×10^{-6} in the 2×2 4-PSK Alamouti 256-QAM with SSD system).

B.1. Introduction

Over the past years, there has been an explosive increase in the demand for communications with high data rates and reliable link margin. Research has shown that multiple-input multiple-output (MIMO) systems can be used to enhance spectral efficiency and increase link quality of wireless communications against multipath fading [1-2]. MIMO systems may be defined as the use of multiple antennas at both the transmitting and receiving ends of a wireless communication link. The concept of MIMO systems is based on improving the overall error performance of wireless communications through spatial diversity and improving the spectral efficiency through spatial multiplexing.

Diversity is a technique used to combat fading by transmitting several replicas of the same information on multiple independent fading channels [3]. One of MIMO systems is the Alamouti scheme. The conventional Alamouti scheme is a space-time block code technique that can achieve full diversity in MIMO wireless communications, with a simple linear maximum-likelihood detection algorithm [4-6].

Signal space diversity (SSD) is another diversity technique which has the potential to achieve the diversity in MIMO wireless communication systems [7-13]. The SSD technique achieves diversity by a two-part notion. First, original symbols are rotated by a certain angle prior to transmission. The objective behind rotation is to transform the signal constellation such that no two components on the same coordinate axis are identical [7-13]. This ensures that any component of any signal point in the signal constellation has sufficient information for symbol identification. The second notion of the SSD technique is to make sure that the components of the rotated signal (in-phase and quadrature phase components) are independently affected by channel fading. This can be achieved by using component interleaving and deinterleaving at the transmitter and the receiver, respectively [7-13]. Hence, the diversity gain in SSD is only achieved after the two conditions have been satisfied (rotation and component interleaving) [7-13].

Based on conventional Alamouti, improved MIMO-Alamouti schemes have been presented by various researchers to try and improve the error performance of wireless communication networks [14, 15]. In [14], Xia and Zhang proposed an Alamouti based Toeplitz STBC to improve the error performance of non-coherent systems in which the channel state information is unavailable at both the transmitter and receiver. Xia and Zhang improved the conventional Alamouti scheme by combining it with the Toeplitz matrix structure in order to enhance the error performance of non-coherent wireless communication systems. Also, in [7, 8], there is published work based on MIMO Alamouti coded M-QAM scheme with SSD. In [8], there is published work by Essop based on MIMO Alamouti coded M-QAM scheme with SSD and generalised selection combining. This scheme uses SSD with Alamouti scheme to another

level of diversity by rotating a constellation twice, thereby decreasing the chances of deep fading and improving the error performance of wireless communication systems.

On the other side, various engineers have presented theories of improving the spectral efficiency of MIMO-Alamouti STBCs [5-6]. In [6], Ling and Li published work on improving the Alamouti code efficiency by expanding the modulation signal set. Unfortunately, a setback on expanding the modulation signal set is the poor bit error rate performance due to reduced minimum Euclidean distance between modulation signals. Hence motivated by the work in Paper A, published work in [6 and 8], a high-rate MIMO Alamouti STBC which incorporates SSD is proposed in this paper. The purpose of the proposed scheme is to further improve the error performance of work in Paper A, whilst retaining the spectral efficiency that was achieved in Paper A with minimum decoding complexity.

The remainder of this paper is structured as follows: Section B.2 presents the proposed N-ary Alamouti M-QAM scheme with SSD, section B.4 presents the theoretical analysis of the BER performance of the system over identical and independently distributed Rayleigh frequency-flat fading channels with AWGN. Section B.5 presents the numerical results and discussion. Finally, the paper is concluded in section B.6.

Notation: For consistent notation, this paper denotes bold lowercase and uppercase letters for vectors and matrices, respectively. Regular letters represent scalar quantities. $\mathbb{C}^{Q\times R}$ is a set of $Q \times R$ complex-valued matrices. $[\cdot]^T, (\cdot)^H, (\cdot)^*, |\cdot|$and $\|\cdot\|_F$ Represent the transpose, Hermitian, conjugate, Euclidean and Frobenius norm operators, respectively. $Q(\cdot)$ is the Gaussian Q-function. $E\{\cdot\}$ is the expectation operator and $\mathrm{argmin}(\cdot)$ and $\mathrm{argmax}(\cdot)$ represent the argument of the minimum or maximum. Finally, $\mathrm{d}^2(x, y)$ represents the squared Euclidean distance between signals *x* and *y*.

B.2. System model

Consider a $2 \times N_R$ N-ary Alamouti scheme with SSD shown in Figure B.2.1. In order for this system to work, information bits are grouped into five bit-streams, $\boldsymbol{b}_i = [b_{i1} b_{i2} \cdots b_{ir}], i \in [1\colon 4], r = \log_2 M$ and $\boldsymbol{b}_5 = [b_{51} b_{52} \cdots b_{5s}], s = \log_2 N$. Bit-stream $\boldsymbol{b}_i$, $i \in [1\colon 4]$, is fed into a Gray-coded mapper which maps r bits into an M-QAM constellation point, and yields a symbol $u_i, i \in [1\colon 4]$ with $E\{|u_i|^2\} = 1$ while bit stream $\boldsymbol{b}_5$ is fed into another Gray-coded mapper which maps s bits into an N-PSK constellation point, and yields a symbol $u_5 = e^{\mathrm{j}\theta_q}, q \in [1\colon N]$ with $E\{|u_5|^2\} = 1$.

Let $\boldsymbol{\Omega}_1, \widetilde{\boldsymbol{\Omega}}_1$ and $\boldsymbol{\Omega}_2$ represent an M-QAM signal set, M-QAM rotated signal set and N-PSK signal set, respectively. $\boldsymbol{\Omega}_1 = \{u_k^I + \mathrm{j}u_k^Q : k = 0,1,\dots,M-1\}$, where u_k^I and u_k^Q are the in-phase and quadrature parts of the signal respectively.

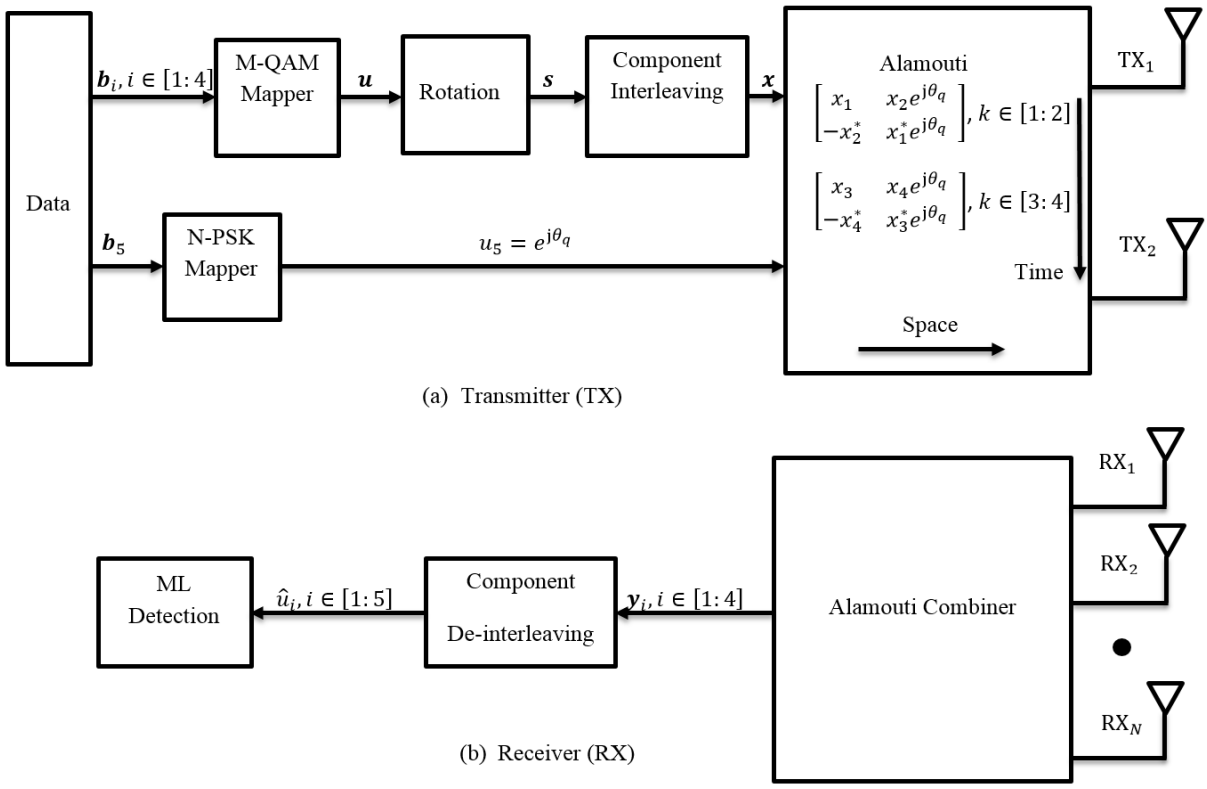

Figure B.2.1: $2 \times N_R$ N-ary Alamouti scheme with SSD system model.

The generated M-QAM symbols $u_i, i \in [1:4]$ are first mapped into a matrix with the in-phase and quadrature components of the signal separated. After that, the M-QAM symbols then undergo rotation by multiplication with a rotation matrix ($\boldsymbol{R}^{\theta_1}$) as shown in (B.2.1-2) to give new rotated symbols ($s_i, i \in [1:4]$).

$$s_i = \begin{bmatrix} u_i^I & u_i^Q \end{bmatrix} \boldsymbol{R}^{\theta_1}, i \in [1:4] \tag{B.2.1}$$

$$\boldsymbol{R}^{\theta_1} = \begin{bmatrix} \cos\theta_1 & \sin\theta_1 \\ -\sin\theta_1 & \cos\theta_1 \end{bmatrix} \tag{B.2.2}$$

where $u_i \in \boldsymbol{\Omega}_1,\ u_i = u_i^I + ju_i^Q; s_i \in \widetilde{\boldsymbol{\Omega}}_1,\ s_i = \begin{bmatrix} s_i^I & s_i^Q \end{bmatrix}$ and $(\cdot)^I, (\cdot)^Q$ are the in-phase and quadrature parts of a signal, respectively. Since it is assumed that $E\{|u_i|^2\} = 1$, we also have $E\{|s_i|^2\} = 1$. $\boldsymbol{R}^{\theta_1}$ is the rotational matrix and θ_1 is the angle of rotation. According to [8, 11, 13], there are two commonly used techniques to derive this angle, namely the minimum product distance (MPD) approach and the

design criteria approach. In [8, 13, 15] it has been shown that the MPD approach results in a better overall performance, hence this scheme applies $\theta_1 = 31.7^{\circ}$ derived using the MPD approach [8, 15].

The unique components of the rotated symbols in (B.2.1) are interleaved to ensure that they are affected by independent and different fading to obtain diversity. Interleaving ensures that a single deep fade will not affect all components of the signal simultaneously. This is achieved using a component interleaver or de-interleaver present at the transmitter and receiver respectively [8, 11, 15]. Component interleaving prior to transmission gives four interleaved symbols $(x_i, i \in [1:4])$ as shown in (B.2.3-4):

$$x_i = s_i^I + \mathrm{j}s_{i+2}^Q \,, \; i \in [1:2] \tag{B.2.3}$$

$$x_i = s_i^I + \mathrm{j}s_{i-2}^Q, \; i \in [3:4] \tag{B.2.4}$$

Based on $E\{|s_i|^2\} = 1$ we further have $E\{|x_i|^2\} = 1$. Then the modified Alamouti scheme with SSD scheme is then given by:

$$\boldsymbol{X}_i = \begin{bmatrix} x_{2i-1} & x_{2i}e^{\mathrm{j}\theta_q} \\ -x_{2i}^* & x_{2i-1}^* e^{\mathrm{j}\theta_q} \end{bmatrix}, \; i \in [1:2] \tag{B.2.5}$$

In $\boldsymbol{X}_1$ the two pairs of rotated and interleaved symbols together with the N-PSK symbol, $\left(x_1, x_2 e^{\mathrm{j}\theta_q}\right)$ and $\left(-x_2^*, x_1^* e^{\mathrm{j}\theta_q}\right)$ are transmitted through transmit antenna one and two in the first two time slots while for $\boldsymbol{X}_2$, the other two pairs of symbols $\left(x_3, x_4 e^{\mathrm{j}\theta_q}\right)$ and $\left(-x_4^*, x_3^* e^{\mathrm{j}\theta_q}\right)$ are transmitted in the second two time slots. We refer to the above transmission scheme as the N-ary Alamouti M-QAM scheme with SSD.

The received signals are given as,

$$\boldsymbol{y}_{2i-1} = \boldsymbol{h}_{2i-1}x_{2i-1} + \boldsymbol{h}_{2i}x_{2i}e^{\mathrm{j}\theta_q} + \boldsymbol{n}_{2i-1}, \; i \in [1:2] \tag{B.2.6}$$

$$\boldsymbol{y}_{2i} = \boldsymbol{h}_{2i-1}(-x_{2i}^*) + \boldsymbol{h}_{2i}x_{2i-1}^* e^{\mathrm{j}\theta_q} + \boldsymbol{n}_{2i}, \; i \in [1:2] \tag{B.2.7}$$

where $l \in [1:4]$, $\boldsymbol{y}_l \in \mathbb{C}^{N_R \times 1}$ is the l^{th} received signal vector, $\boldsymbol{h}_l \in \mathbb{C}^{N_R \times 1}$ is the l^{th} channel fading vector, and $\boldsymbol{n}_l \in \mathbb{C}^{N_R \times 1}$ is the l^{th} received additive white Gaussian (AWGN) noise vector. It is assumed that $\boldsymbol{h}_l$ is a quasi-static frequency flat-Rayleigh fading channel. $\boldsymbol{h}_l$ remains the same value in two-time slots and takes an independent value in other two-time slots. The entries of $\boldsymbol{n}_l$ and $\boldsymbol{h}_l$ are independent and identically distributed (i.i.d) Gaussian random variables (RVs), which follow the distributions $CN(0,2/\rho)$ and $CN(0,1)$, respectively. $\frac{\rho}{2}$ is the average signal-to-noise ratio (SNR) at each receive antenna.

B.2.2. Detection

Based on [9, 12, 17, 20], it is assumed that full channel state information (CSI) is known at the receiver and the detection process is done using the following steps.

Step 1: Given $u_5 = e^{\mathrm{j}\theta_q}, q \in [1:N]$ first, calculate the following;

$$\boldsymbol{H}_{2w}(u_5) = \boldsymbol{h}_{2w}e^{\mathrm{j}\theta_q}, w \in [1:2] \tag{B.2.8}$$

$$g_1(u_5) = (\|\boldsymbol{h}_1\|_F^2 + \|\boldsymbol{h}_2\|_F^2) \tag{B.2.9}$$

$$g_2(u_5) = (\|\boldsymbol{h}_3\|_F^2 + \|\boldsymbol{h}_4\|_F^2) \tag{B.2.10}$$

where $\boldsymbol{H}_{2w}(u_5) \in \mathbb{C}^{4\times 1}$ and $w \in [1:2]$.

Step 2: The received signals in (B.2.6) and (B.2.7) are sent to the combiner and are multiplied by step 1 results to give the outputs of the combiner as;

$$\tilde{Z}_{2w-1}(u_5) = (\boldsymbol{h}_{2w-1}^H)(\boldsymbol{y}_{2w-1}) + (\boldsymbol{y}_{2w}^H)(\boldsymbol{H}_{2w}), w \in [1:2] \tag{B.2.11}$$

$$\tilde{Z}_{2w}(u_5) = (\boldsymbol{H}_{2w}^H)(\boldsymbol{y}_{2w-1}) - (\boldsymbol{y}_{2w}^H)(\boldsymbol{h}_{2w-1}), w \in [1:2] \tag{B.2.12}$$

where $\widetilde{Z}_w(u_5) \in \mathbb{C}^{1\times 1}, w \in [1:4]$ are the outputs of the combiner.
(B.2.11) and (B.2.12) can be further rewritten as;

$$\tilde{Z}_{2w-1}(u_5) = \tilde{Z}_{2w-1}^I(u_5) + \mathrm{j}\tilde{Z}_{2w-1}^Q(u_5),\ w \in [1:2] \tag{B.2.13}$$

$$\tilde{Z}_{2w}(u_5) = \tilde{Z}_{2w}^I(u_5) + \mathrm{j}\tilde{Z}_{2w}^Q(u_5),\ w \in [1:2] \tag{B.2.14}$$

where $\widetilde{Z}_l^I(u_5)$ and $\tilde{Z}_l^Q(u_5),\ l \in [1:4]$ are the in-phase and quadrature parts respectively.

Step 3: The outputs of the combiner from (B.2.13) and (B.2.14) are then sent to the MLD where the N-PSK and M-QAM symbols decoupling, de-interleaving and estimation processes happen [19-26]. For each given N-PSK symbol $u_5 = e^{\mathrm{j}\theta_q}$, the four transmitted M-QAM symbols are detected using MLD and the estimated four candidate symbols $(\hat{u}_i(u_5), i \in [1:4])$ are given as;

$$\hat{u}_1(u_5) = \underset{x_k \in \widetilde{\boldsymbol{\Omega}}_1}{\operatorname{argmin}}\{(B)(C) + (A)(D)\} \tag{B.2.15}$$

$$\hat{u}_2(u_5) = \underset{x_k \in \widetilde{\boldsymbol{\Omega}}_1}{\operatorname{argmin}}\{(B)(E) + (A)(F)\} \tag{B.2.16}$$

$$\hat{u}_3(u_5) = \underset{x_k \in \widetilde{\Omega}_1}{\operatorname{argmin}}\{(A)(G) + (B)(L)\} \tag{B.2.17}$$

$$\hat{u}_4(u_5) = \underset{x_k \in \widetilde{\Omega}_1}{\operatorname{argmin}}\{(A)(T) + (B)(R)\} \tag{B.2.18}$$

where; $A = (\|\boldsymbol{h}_1\|_F^2 + \|\boldsymbol{h}_2\|_F^2), B = (\|\boldsymbol{h}_3\|_F^2 + \|\boldsymbol{h}_4\|_F^2), C = \left|Ax_k^I - \tilde{Z}_1^I\right|^2,\ D = \left|Bx_k^Q - \tilde{Z}_3^Q\right|^2,$

$$E = \left|Ax_k^I - \tilde{Z}_2^I\right|^2, F = \left|Bx_k^Q - \tilde{Z}_4^Q\right|^2, G = \left|Bx_k^I - \tilde{Z}_3^I\right|^2, L = \left|Ax_k^Q - \tilde{Z}_1^Q\right|^2, T = \left|Bx_k^I - \tilde{Z}_4^I\right|^2$$

and $R = \left|Ax_k^Q - \tilde{Z}_2^Q\right|^2$.

Step 4: The four estimated M-QAM symbols $(\hat{u}_i(u_5), i \in [1:4])$ in step 3, are assumed to be correctly detected and the next step is to calculate the following metric distance $\big(D(u_5)\big)$ as follows;

$$D(u_5) = \sum_{i=1}^{4} d_i\,(u_5), i \in [1:4] \tag{B.2.19}$$

where $d_{2i-1}(u_5) = \left\|\boldsymbol{y}_{2i-1} - (\boldsymbol{h}_{2i-1})\big(\hat{u}_{2i-1}(u_5)\big) - (\boldsymbol{h}_{2i})\big(\hat{u}_{2i}(u_5)\big)(u_5)\right\|_F^2, i \in [1:2]$

and $d_{2i}(u_5) = \left\|\boldsymbol{y}_{2i} - (\boldsymbol{h}_{2i-1})\big(-\hat{u}_{2i}^*(u_5)\big) - (\boldsymbol{h}_{2i})\big(\hat{u}_{2i-1}^*(u_5)\big)(u_5)\right\|_F^2, i \in [1:2]$.

Step 5: Steps 1 up to 4 are repeated N times, thereby giving N values of the metric distance $D_l(u_5), l \in [1:N]$ which are stored in a $1 \times N$ matrix $\big(\mathbf{F}(u_5)\big)$.

Step 6: Finally, the estimation of the M-PSK symbol is done by minimising the following ML metric.

$$\tilde{u}_5 = \underset{e^{j\theta_q}, \tilde{x}_i = \hat{x}_i(\,x_5) \in \boldsymbol{\Omega}_3}{\operatorname{argmin}} \big(\mathbf{F}(u_5)\big) \tag{B.2.20}$$

where $\tilde{u}_5 = e^{j\widehat{\theta}_q}$ is the estimation of the M-PSK symbol and $\boldsymbol{\Omega}_3$ is the set containing the estimated M-QAM symbols $\hat{u}_i, i \in [1:4]$ and the given $\big(u_5 = e^{j\theta_q}\big)$ value.

B.3. Error Performance Analysis

The previously discussed detection above, in section (B.2.2), is a joint detection. There are two types of errors in the above detection. One is the error of estimating the N-PSK symbol while the other one is the error in estimating M-QAM symbols. However, it is not easy to derive the whole error probability of the joint detection. In this section, we only consider the low error performance bound of the joint detection. That is, we only consider the error probability of estimating M-QAM symbols using the

nearest neighbourhood (NN) approach based on Euclidean distance (ED), given that the N-PSK symbol is perfectly detected. Let P_d denote the average bit error probability (ABEP) of estimating M-QAM symbols given that the N-PSK symbol is perfectly detected. The low error probability bound of the proposed system is given by

$$P_e \geq P_d \tag{B.3.1}$$

Given that the N-PSK symbol $\left(e^{\mathrm{j}\theta_q}\right)$ is perfectly detected at the receiver then the equivalent received signal may be written as

$$\boldsymbol{y}_{2v-1} = \boldsymbol{h}_{2v-1}x_{2v-1} + \boldsymbol{H}_{2v}x_{2v} + \boldsymbol{n}_{2v-1},\ v \in [1:2] \tag{B.3.2}$$

$$\boldsymbol{y}_{2v} = \boldsymbol{h}_{2v-1}(-x_{2v}^{*}) + \boldsymbol{H}_{2v}x_{2v-1}^{*} + \boldsymbol{n}_{2v},\ v \in [1:2] \tag{B.3.3}$$

where $\boldsymbol{H}_{2v}, v \in [1:2]$ are known at the receiver.

N-ary Alamouti M-QAM with SSD may be viewed as a $2 \times N_R$ MIMO configuration and in [25, 27, 21-29], it was shown that an Alamouti scheme with N_R receive antennas is equivalent to an MRC system with $2N_R$ receive antennas and half transmission power used. Fortunately, the BEP (P_d) of M-QAM symbols using the NN approximation has already been done before in the literature [8, 12, 13]. Hence, the low bound bit error probability (BER) of the proposed system using NN approximation with N_R-branch receive MRC over Rayleigh fading channels is given in [8, 15] as;

$$P_d(\rho) = P_{SER\ M-QAM}^{NN}(e) = A_M P[X_A \to X_B]_{AL} + B_M P[X_A \to X_C]_{AL} \tag{B.3.4}$$

$$P_d(\rho) = P_{BER\ M-QAM}^{NN}(e) = \frac{1}{r}\left[A_M P_{perp}(x \to \hat{x}) + B_M P_{diag}(x \to \hat{x})\right] \tag{B.3.5}$$

where A_M and B_M are the coefficients of the pairwise error probabilities (PEPs) and are found in table B.3.1 below as discussed in [8, 15]. These represent the number of immediate perpendicular and diagonal neighbours of the described points with different Euclidean distances. $P_{perp}(x \to \hat{x})$ and $P_{diag}(x \to \hat{x})$ are equivalent to $P[X_A \to X_B]_{AL}$ and $P[X_A \to X_C]_{AL}$, respectively. These are the perpendicular and diagonal PEPs between any described point and its perpendicular and diagonal neighbours respectively. The derivation of the PEPs is discussed in [29] and is given as

$$P(x \to \hat{x}) = \int_0^\infty \int_0^\infty Q\left(\sqrt{\frac{1}{2E_s}(\gamma_1^2 Đ_1^2 + \gamma_2^2 Đ_2^2)}\right) f_{\gamma MRC}(\gamma_1) f_{\gamma MRC}(\gamma_2)\, d\gamma_1\, d\gamma_2 \tag{B.3.6}$$

where $Đ_i^2, i \in [1:2]$ are the distances for perpendicular and diagonal neighbours given in table B.3.2, E_s is the average expected energy per symbol and is calculated based on the M-QAM constellation size. $\gamma_i,\ i \in [1:2]$ is the SNR, $\bar{\gamma} = \rho$ is the average SNR and $f_{\gamma MRC}(\gamma_i), i \in [1:2]$ is the MRC PDF for multiple receivers (N_R) and it is given in [15] as

$$f_{\gamma MRC}(\gamma_i) = \frac{1}{(N_R-1)!}\frac{1}{\bar{\gamma}^{N_R}}\gamma_i{}^{N_R-1}e^{\left(-\frac{\gamma_i}{\bar{\gamma}}\right)} \quad \text{(B.3.7)}$$

16-QAM examples of the derived PEPs are given in [8, 15] as

$$P_{perp}(x \to \hat{x}) = \frac{1}{4n}M_1M_2 + \frac{1}{2n}\sum_{k=1}^{n-1}M_3M_4 \quad \text{(B.3.8)}$$

$$P_{diag}(x \to \hat{x}) = \frac{1}{4n}M_5M_6 + \frac{1}{2n}\sum_{k=1}^{n-1}M_7M_8 \quad \text{(B.3.9)}$$

Where $M_1 = (1 + 0.145\bar{\gamma}_I)^{-N_R}, M_2 = \left(1 + 0.055\bar{\gamma}_Q\right)^{-N_R}, M_3 = \left(\frac{S_i+0.145\bar{\gamma}_I}{S_i}\right)^{-N_R}$,

$M_4 = \left(\frac{S_i + 0.055\bar{\gamma}_I}{S_i}\right)^{-N_R}, M_5 = (1 + 0.021\bar{\gamma}_I)^{-N_R}, M_6 = (1 + 0.379\bar{\gamma}_I)^{-N_R}$,

$M_7 = \left(\frac{S_i+0.021\bar{\gamma}_I}{S_i}\right)^{-N_R}, M_8 = \left(\frac{S_i+0.379\bar{\gamma}_I}{S_i}\right)^{-N_R}, S_i = 2(\sin\beta_i)^2, \beta_i = \frac{i\pi}{4n}$ and n is the number of iterations used in the approximation.

Table B.3.1: Values for A_M, B_M and E_S

Constellations	A_M	B_M	E_S
4	2	1	2
16	3	2.25	10
64	3.5	3.51	42
256	3.75	3.5156	170

Table B.3.2: Perpendicular and diagonal distances for the pairwise error probabilities.

Perpendicular distances	Diagonal distances
$Ð^2_{1perp} = 4\cos^2\theta_1$	$Ð^2_{1diag} = 4(1 + \sin(2\theta_1))$
$Ð^2_{2perp} = 4\sin^2\theta_1$	$Ð^2_{2diag} = 4(1 - \sin(2\theta_1))$

B.5. Simulation and numerical results

The aim of this section was to validate the analytical performance developed in (B.3.5) and then provide an error performance comparison between the various N-ary Alamouti M-QAM with SSD schemes. Monte Carlo simulations were performed over i.i.d Rayleigh flat fading channels with AWGN, where the ABEP was plotted against the average SNR at each receive antenna. The parameters regarding the AWGN and channels were consistent with those defined in section B.2.2. The following were assumed during the simulation: Gray coded M-QAM and Gray coded N-PSK constellations; full CSI knowledge at the receivers; signal paths were statistically independent of each other, meaning the channels were uncorrelated [18 and 27] and total transmit power was the same for all transmissions.

Figures B.5.1 - B.5.2 below, show the analytical and simulated ABEP results of the 2×2 and 2×4 (4-PSK, 8-PSK and 16-PSK) Alamouti SSD 16-QAM systems together with the 2×2 and 2×4 Alamouti SSD 16-QAM without PSK system results. In the 2×4 results, it is evident that the theoretical predictions closely predicted the BER performance in the high SNR region. It is also shown that 2×4 (4-PSK, 8-PSK and 16-PSK) Alamouti SSD 16-QAM systems have closely the same BER performance as the 2×4 Alamouti SSD 16-QAM without PSK systems. However, the proposed scheme is more spectral efficient compared to the standard 2×4 Alamouti SSD 16-QAM without PSK systems. The proposed scheme has more data throughput with five symbols sent (more bits sent) whereas the 2×4 Alamouti SSD 16-QAM without PSK systems have only four symbols sent (fewer bits sent). An example of improved spectral efficiency is seen in 16-PSK Alamouti 16-QAM with SSD, which has a high spectral efficiency of 1.5 bits/sec/Hz as compared to 1 bit/sec/Hz 16-QAM Alamouti scheme. These values were calculated with the aid of eq (2.1) and table B.5.5, where $N_T = 2, \tau = 4$ and the number of bits depends on the system concerned (4 bits for 16-QAM Alamouti scheme and 8 bits for 16-PSK Alamouti 16-QAM with SSD). Hence the proposed 2×4 N-ary Alamouti SSD scheme exhibits an improved higher bandwidth efficiency.

The next set of results (Figures B.5.3 - B.5.6) below, show the analytical and simulated ABEP results of various 2×2 and 2×4 N-ary Alamouti SSD 64 and 256-QAM systems. Like Figures B.5.1-4, the results show clearly that the theoretical closely predicts the BER performance in the high SNR region. Also, it is seen that 2×4 N-ary Alamouti SSD 64 and 256-QAM schemes have the same BER performance as 2×4 Alamouti 64 and 256-QAM without PSK schemes. This is an improvement in data throughput as they have more symbols (more bits) sent than the 2×4 standard Alamouti SSD M-QAM schemes without PSK (fewer bits sent). From the results, there is more spectral efficiency in the proposed N-ary Alamouti M-QAM scheme as compared to the standard Alamouti SSD schemes without PSK. An example of improved spectral efficiency is seen in 16-PSK Alamouti 64-QAM with SSD,

which has a high spectral efficiency of 1.7 bits/sec/Hz as compared to 1.3 bits/sec/Hz 64-QAM Alamouti scheme. These values were calculated with the aid of eq (2.1) and table B.5.6, where $N_T = 2, \tau = 4$ and the number of bits depends on the system concerned (6 bits for 64-QAM Alamouti scheme and 10 bits for 16-PSK Alamouti 16-QAM with SSD).

However, it can also be seen from the results that error performance together with the accurate prediction of theoretical analysis, improves with the increasing number of receivers. This is seen from the 2×2 results of 16 QAM which have a poor error performance and their theoretical analysis do not closely match the simulated results as compared to the 2×4 results. Hence with an increase in modulation order (M and N), the better the simulation results closely follow the theoretical analysis. This is seen with 2×2 systems of 64 QAM and 256 QAM. Also, an increase in the number of receivers leads to an improvement in the BER performance. Evidence of improvement in BER performance is seen in 256QAM systems at 20 dB SNR where an improvement in BER of 1×10^{-2} in the 2×4 system is seen as compared to a higher BER of 4.31×10^{-2} at the same SNR seen in the 2×2 system. This is because of the increase in receivers. Multiple receivers and higher modulation orders mean more receive diversity and increase in the signal-to-noise-ratio at the destination. This, in turn, leads to an improved error performance [30].

The last set of results (Figure B.5.7) show 2×4 N-ary Alamouti vs N-ary Alamouti with SSD schemes. In the results, there is an improvement in the BER performance of N-ary Alamouti with SSD as compared to that of 2×4 N-ary Alamouti without SSD schemes. 4-PSK Alamouti SSD 256-QAM showed 0.8 dB improvement at a BER of 1.06×10^{-6} as compared to 4-PSK Alamouti 256-QAM without SSD. Similar results were seen in 8-PSK Alamouti SSD 16 QAM with an improvement of 1 dB compared to that of 8-PSK Alamouti without SSD 16QAM at a BER of 1.06×10^{-6}. These results show that SSD is an extremely spectral and power efficient method of increasing the error performance of a system, as it efficiently reduced the N-ary Alamouti schemes error performance by 0.8 dB overall. However, the only expense incurred is the slight increase in the complexity of the MLD detection.

Table B.5.7: N-ary Alamouti with SSD spectral efficiency values.

QAM constellation	PSK constellation	Standard Alamouti bits sent	N-ary Alamouti bits sent	Standard Alamouti spectral efficiency (bits/sec/Hz)	N-ary Alamouti spectral efficiency (bits/sec/Hz)
16	4	4	6	1	1.3
16	8	4	7	1	1.4
16	16	4	8	1	1.5
32	4	5	7	1.2	1.4
32	8	5	8	1.2	1.5
32	16	5	9	1.2	1.6
64	4	6	8	1.3	1.5
64	8	6	9	1.3	1.6
64	16	6	10	1.3	1.7
256	4	8	10	1.5	1.7
256	8	8	11	1.5	1.7
256	16	8	12	1.5	1.8

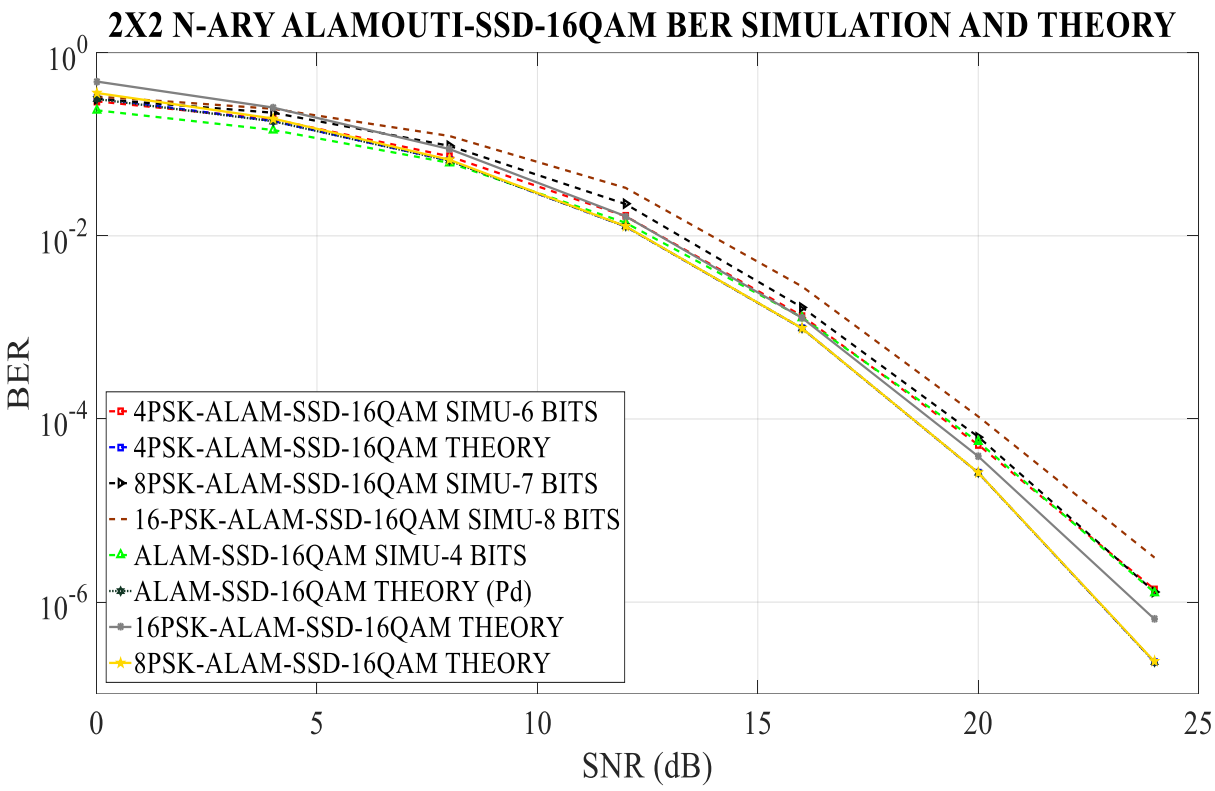

Figure B.5.1: 2 × 2 N-ary Alamouti SSD 16-QAM results.

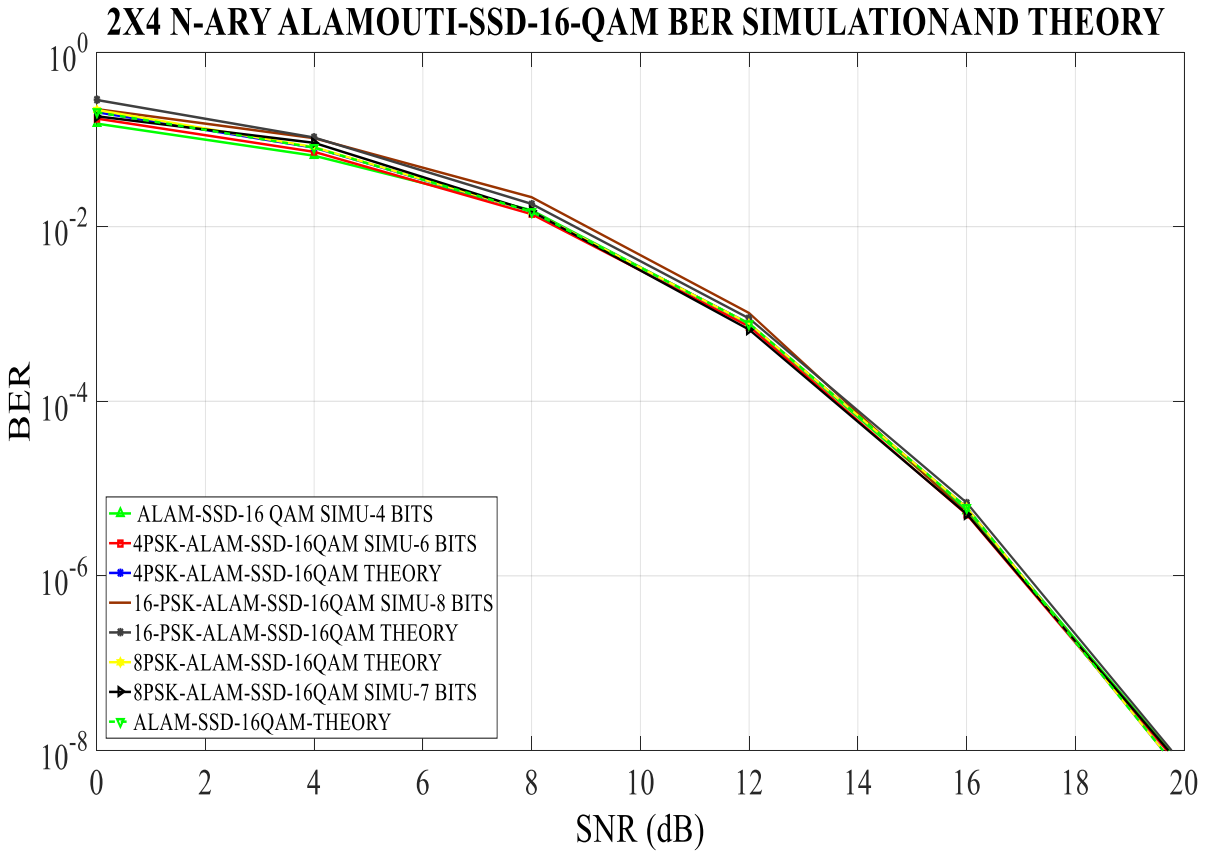

Figure B.5.2: 2 × 4 N-ary Alamouti SSD 16-QAM results.

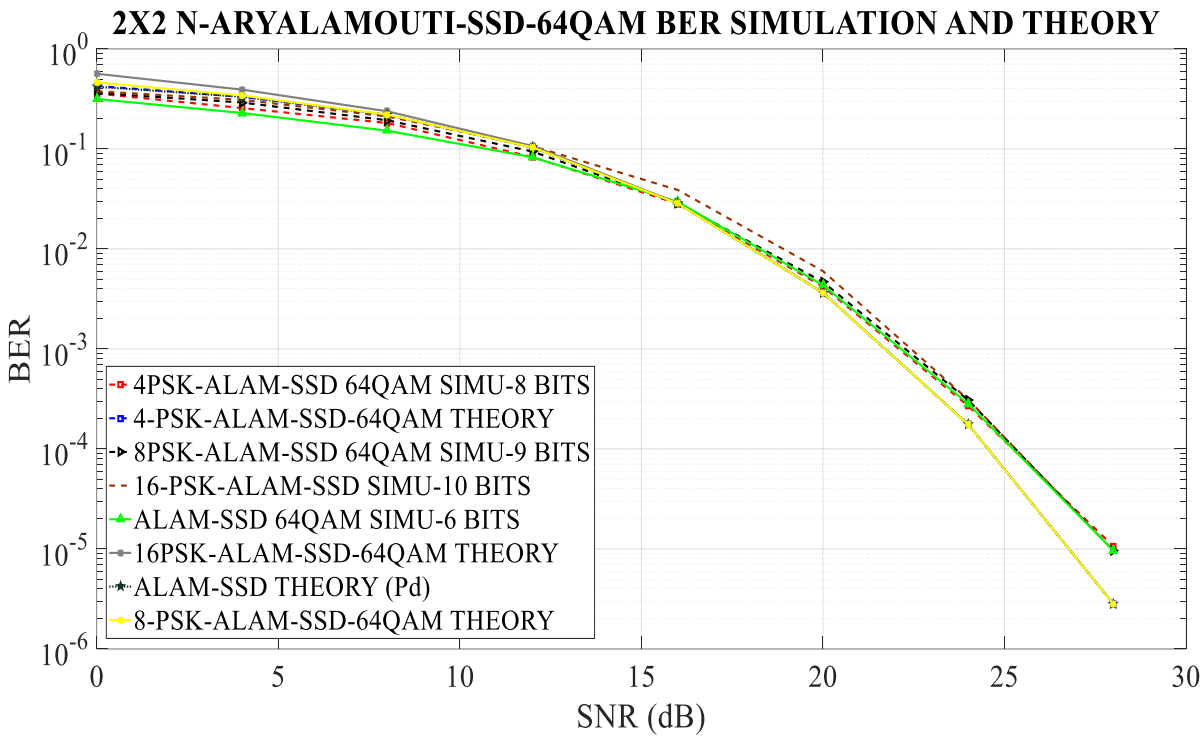

Figure B.5.3: 2 × 2 N-ary Alamouti SSD 64-QAM results.

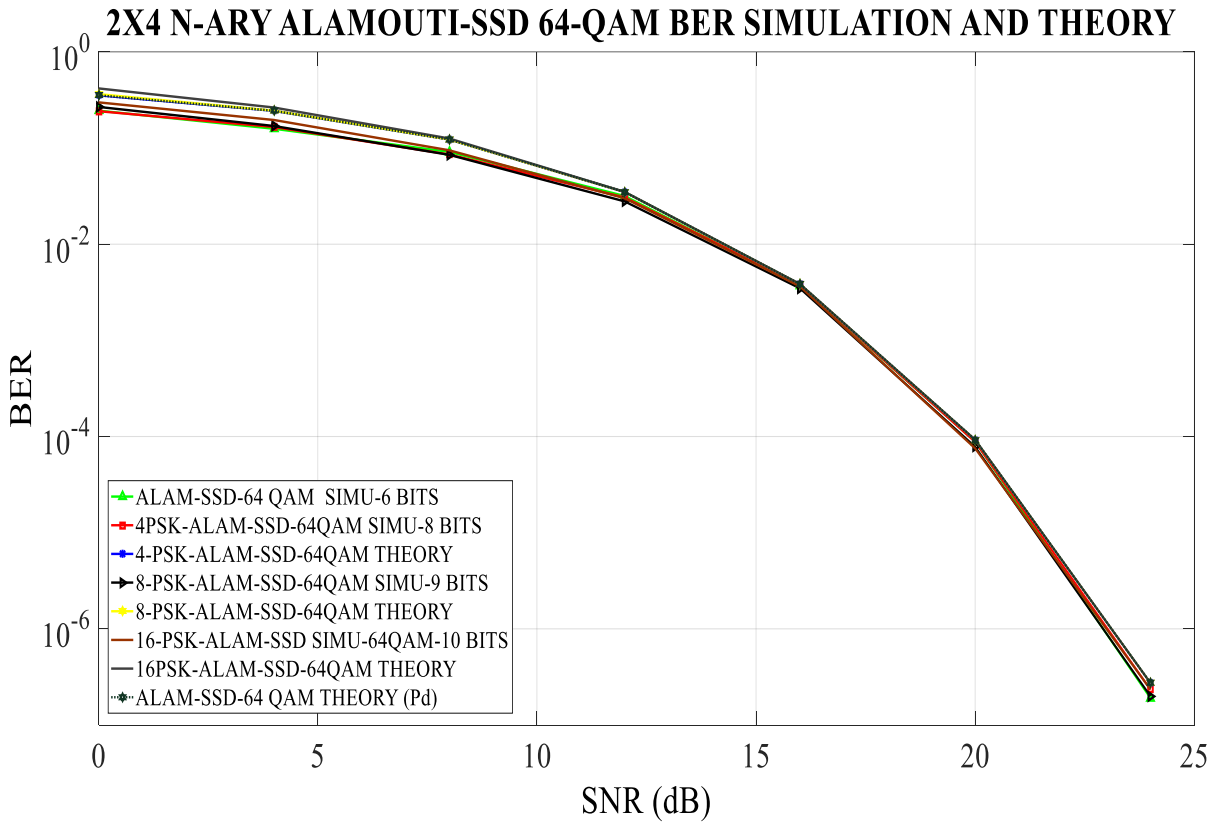

Figure B.5.4: 2 × 4 N-ary Alamouti SSD 64-QAM results.

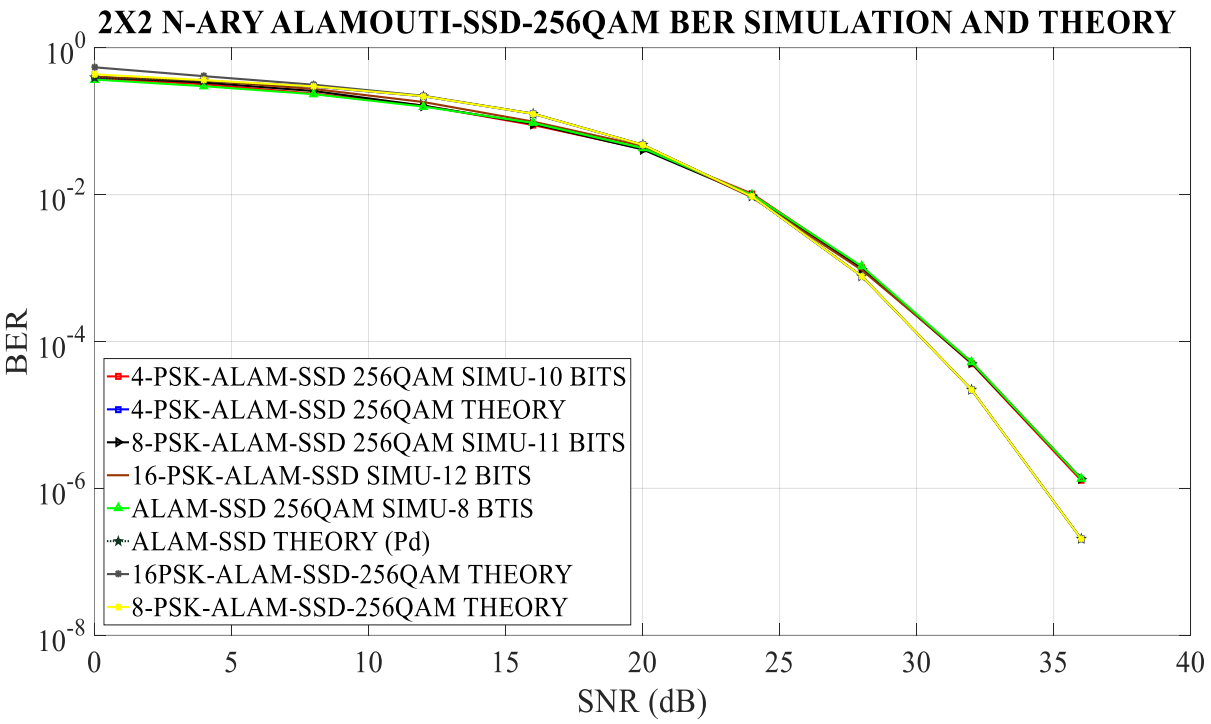

Figure B.5.5: 2×2 N-ary Alamouti SSD 256-QAM results.

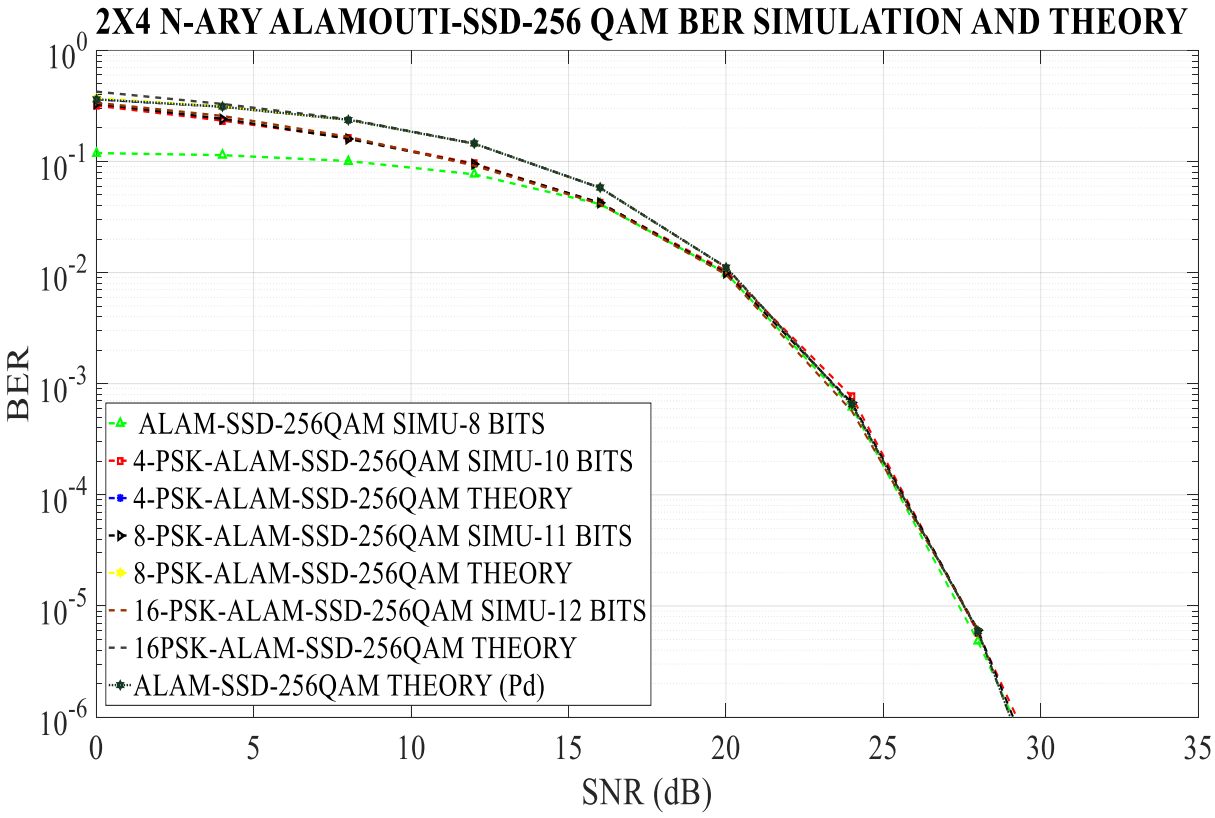

Figure B.5.6: 2×4 N-ary Alamouti SSD 256-QAM results.

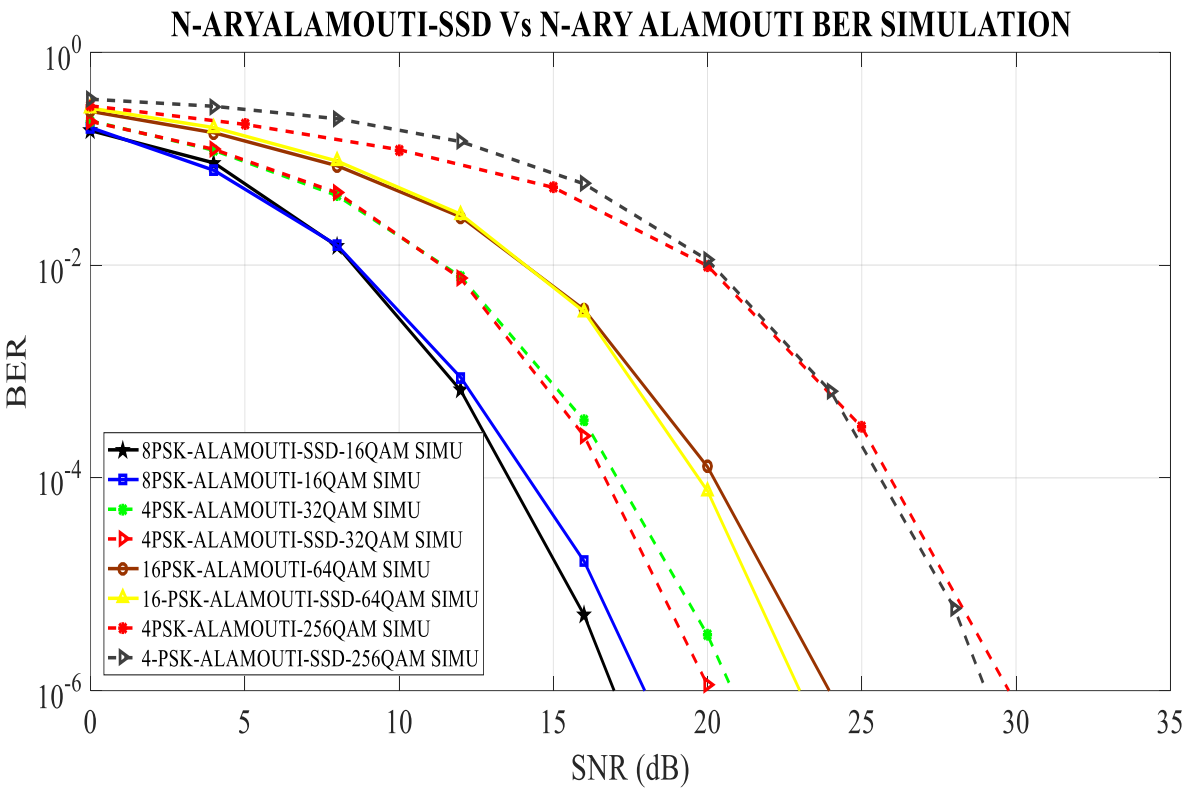

Figure B.5.7: M-ary Alamouti vs M-ary Alamouti with SSD comparison of results.

B.6. Conclusion

In this paper, the error performance and spectral efficiency of N-ary Alamouti with SSD system were investigated. The study is restricted to 2×2 and 2×4 systems of (4-PSK, 8-PSK and 16-PSK) Alamouti SSD (16, 64 and 256 QAM) schemes. An analytical ABEP expression was derived and validated against simulated results. It was shown to converge to simulation results in the high SNR region. Results presented indicate increased spectral efficiency in the proposed scheme but with a tight matching BER performance as the standard 2×4 Alamouti M-QAM with SSD systems. Also, the results show that the proposed scheme is more spectrally efficient and has a better BER performance (0.8 dB improvement) compared to the standard 2×4 Alamouti M-QAM without SSD systems discussed in paper A. It was also found that the BER performance of the proposed scheme, improved with an increase in the number receivers.

B.7. References

[1] A. A. Kwabena, *Multiple Input Multiple Output (MIMO) Operation Principles,* Finland: Helsinki Metropolia University Of Applied Sciences, Thesis published, 2013.

[2] A. Krumbein, "White Paper: Understanding the basics of MIMO communication Technology," 1 November 2016. [Online]. Available: https://www.southwestantennas.com/white-paper-understanding-basics-mimo-communication-technology. [Accessed 16 February 2018].

[3] C. K. Agubor, F. K. Opara and G. N. Eze, "A Review of Diversity Techniques for Wireless Communications," *Academic Research International (ARInt.),* vol. 4, no. 2, pp. 157-167, 2013.

[4] S. Alamouti, "A Simple Transmit Diversity technique for wireless Communications," *IEEE, Selected Areas on Communications,* vol. 16, no. 8, pp. 1451-1458, 1998.

[5] Z. A. Baloch, M. U. Baloch and N. Hussain, "Efficiency improvement of space-time block codes," *International Journal of Coomun Net and Syst Sci,* vol. 3, no. 6, pp. 507-510, 2010.

[6] Q. Ling and T. Li, "Efficiency improvement for Alamouti codes," in *IEEE 40th Annual Conference on Information Sciences and Systems,* Princeton, New Jersey, USA, pp. 569-572. 2006.

[7] A. Saed, H. Xu and T. Quazi, "Alamouti Space-time Block coded Hierarchical Modulation with Signal Space Diversity and MRC reception in Nakagami-m fading channels," *IET Communications,* vol. 8, no. 4, pp. 516-524, 2013.

[8] A. Essop and H. Xu, "Alamouti Coded M-QAM with Single and Double Rotated Signal Space Diversity and generalised selection Combining Reception in Rayleigh Fading Channels," *SAIEE Africa Research Journal,* vol. 100, no. 3, pp. 221-223, 2015.

[9] J. Taejin and C. Kyungwhoon, "Design of Concatenated Space-Time Block Codes Using Signal Space Diversity and the Alamouti Scheme," *IEEE Communications Letters,* vol. 7, no. 7, pp. 329-331, 2003.

[10] S. Jeon, J. Lee, I. Kyung and M. K. Kim, "Component-interleaved Alamouti coding with Rotated Constellations for Signal Space Diversity," *IEEE International Symposium on Broadband Multimedia Systems and Broadcasting,* vol. 1, no. 1, pp. 1-6, 2010.

[11] J. Boutros and E. Viterbo, "Signal Space Diversity: A Power and Bandwidth-efficient Diversity Technique for the Rayleigh Fading channel," *IEEE Transactions on Information Theory*, vol. 1, no. 1, p. 1453, Jul. 1998.

[12] H. Zhao, H. Wang, J. Kuang, Z. Fei and C. Yan, "Improved coded Cooperation scheme with Signal Space Diversity in wireless networks," in *International Conference on Wireless Communications and Signal Processing*, pp. 1-6. 2009.

[13] A. Seyed, S. Ahmadzadeh, M. Abolfazl and K. K. Amir, "Signal Space Cooperative communication," *IEEE Transactions on Wireless Communications*, vol. 1, no. 1, pp. 1266-1271, April. 2010.

[14] D. Xia, J. K. Zhang, S. Dumitrescu and F. K. Gong, "Full Diversity non-coherent Alamouti-based Toeplitz Space-Time Block Codes," *IEEE Transactions Signal Processes*, vol. 60, no. 1, pp. 5241-5253, 2012.

[15] H. Xu and Z. Paruk, "Perfomance Analyisi and Simplified Detection for Two-Dimensional Signal Space Diversity with MRC Reception," *SAIEE*, vol. 104, no. 3, pp. 101-102, 2013.

[16] J. Kaur, M. L. Singh and R. S. Sohal, "Performance of Alamouti scheme with convolution for MIMO system," in *2nd International Conference on Recent Advances in Engineering Computational Sciences (RAECS)*, 2015.

[17] Z. Chen, J. Yuan, B. Vucetic and Z. Zhou, "Performance of Alamouti Scheme with transmit antenna selection," *IEE Electronic Letters*, vol. 39, no. 1, pp. 1666-1668, November. 2003.

[18] T. Jung and K. Cheun, "Design of Concatenated space-Time Block codes using Signal Diversity and the Alamouti Scheme," *IEEE Communication Letters*, vol. 7, no. 7, pp. 329-331, July. 2003.

[19] T. Liew and L. Hanzo, "Space-Time Codes and Concatenated channel Codes for wireless communications," *Proceedings of the IEEE*, vol. 90, no. 2, pp. 187-219, February. 2002.

[20] K. K. Wong, "Performance Analysis of Single and Multiuser MIMO Diversity Channels Using Nakagami-m Distribution," *IEEE Transactions on Wireless Communications*, vol. 3, no. 4, pp. 1043-1047, 2004.

[21] N. F. Kiyani, J. H. Weber, A. G. Zajr and G. L. Stuber, "Performance Analysis of a System using Cordinate Interleaving and constelation Rotation in Rayleigh Fading Channels," in *IEEE Conference Vehicular Technonology*, Calgary, Canada, pp. 1-5, 2008.

[22] S. Jeon, I. Kyung and M. S. Kim, "Component-Interleaved Receive MRC with Rotated Constellation for Signal Space Diversity," in *70th IEEE Semi-Annual Vehicular Technology Conference (IEEE VTC 2009- Fall)*, Anchorage, Alaska, USA, September, 2009.

[23] J. H. Winters, "The Diversity gain of Transmit Diversity in wireless systems with Rayleigh Fading," *IEEE ICC*, vol. 2, no. 1, pp. 1121-1125, 1994.

[24] N. Seshadri, "Two Signallling schemes for improving the error performance of FDD transmission systems using transmitter Diversity," *IEEE Vehicular Techonology*, vol. 1, no. 1, pp. 508-511, 1993.

[25] M. Rindani and N. Rindani, "Perfomance improvement of 4X4 Extended Alamouti Scheme with implementation of Eigen Beamforming," *IJCA*, vol. 119, no. 1, pp. 975-1000, 2015.

[26] M. Panthania and V. Bhatia, "BER Aanalysis of STBC Alamouti's Code for MIMO Sytems," *SSRG-IJECE*, vol. 2, no. 7, pp. 2348-2354, 2015.

[27] J. Jeganathan, A. Ghrayeb and L. Szczecinski, "Spatial Modulation: Optimal Detection and Performance Analysis," *IEEE Commun Letters*, vol. 12, no. 8, pp. 545-547, 2008.

[28] I. AL-Shahrani, "Performance of M-QAM Over generalised Mobile Fading Channels Using MRC Diversity," MSc Published Thesis, King Saud University, RIA, Saudi Arabia, 2007.

[29] H. Xu, "Symbol Error Probability for Generalised Selection Combining Reception of M-QAM," *SAIEEE Africa Research Journal*, vol. 100, no. 3, pp. 68-71, 2009.

[30] S. Tarun, I. Kaur and B. Pahwa, "Simplified processing for high-efficiency wireless communication employing multiple antenna aarays," *IJCA*, vol. 87, no. 16, pp. 31-35, 2014.

Part III

Conclusion and future work

MIMO-Alamouti scheme-based systems offer transmit antenna diversity to better the overall diversity of a wireless communication link. These MIMO-Alamouti scheme-based systems manage to offer diversity to a wireless communication link, at the expense of spectral efficiency. This study attempted to improve both the spectral efficiency and the error performance of MIMO-Alamouti scheme-based systems using high modulation techniques (QAM and PSK) with Signal Space Diversity. The results are presented in two papers contained in this dissertation.

In paper A, an $N_T \times N_R$ N-ary Alamouti (M-QAM) scheme was introduced. It is an STBC that aims to improve bandwidth efficiency in MIMO wireless communications. A theoretical BER expression was derived and the derived analytical expression was validated with Monte-Carlo simulations. Bandwidth efficiency increases were seen in the results where the 2×4 N-ary Alamouti M-QAM systems had the same BER performance but with higher data throughput as compared to 2×4 Alamouti M-QAM systems without PSK. There was an improvement in the spectral efficiency of the 16-PSK Alamouti 16-QAM, which had a high spectral efficiency of 1.5 bits/sec/Hz as compared to 1 bit/sec/Hz of 16-QAM Alamouti scheme without PSK.

In paper B, an $N_T \times N_R$ N-ary Alamouti M-QAM scheme with Signal Space Diversity was introduced. It is an expansion of the work in paper A. This scheme incorporated N-PSK, M-QAM, Alamouti and SSD. NN approximation using low error probability bound approach was used to derive the BER expression of the proposed scheme. Simulation results validated the theoretical BER expression for various N-PSK and M-QAM schemes. The results exhibited the same bandwidth efficiency improvement as that of paper A. However, in addition, paper B proposed scheme showed an improvement in the error performance of the schemes compared to those of paper A. There was an improvement in the BER performance of N-ary Alamouti with SSD as compared to that of 2×4 N-ary Alamouti without SSD schemes. 4-PSK Alamouti SSD 256-QAM showed 0.8 dB improvement at a BER of 1.06×10^{-6} as compared to 4-PSK Alamouti 256-QAM without SSD.

In conclusion, the proposed schemes in this dissertation highlighted an insight to the improvement of spectral efficiency and BER performance in wireless communications. For future work, the proposed schemes could be investigated over different fading channels and they could also be used together with spatial modulation (SM) schemes, energy-managing schemes and with hierarchical coding to provide error protection.